C.P. No. 1363

C.P. No. 1363

PROCUREMENT EXECUTIVE, MINISTRY OF DEFENCE

AERONAUTICAL RESEARCH COUNCIL

CURRENT PAPERS

The Current State of Research and Design in High Pressure Ratio Centrifugal Compressors

by

P. M. Came

LONDON: HER MAJESTY'S STATIONERY OFFICE

1977

£3 net

CP No.1363*
July 1976

THE CURRENT STATE OF RESEARCH AND DESIGN IN HIGH PRESSURE RATIO CENTRIFUGAL COMPRESSORS**

by

P.M. Came

SUMMARY

A review of the achievements of research effort in centrifugal compressors is presented and its effect on current design methods is discussed. The paper concludes with recommendations for future research.

---

*Replaces NGTE Note No. NT 1029

**Lecture given at Newcastle University, 24th February 1976

CONTENTS

ILLUSTRATIONS

ILLUSTRATIONS (cont'd)

1.0 Introduction

The use of the centrifugal compressor in gas turbines for aircraft propulsion dates from the first jet engine designed by Whittle. The development of the centrifugal for this role was continued both in Britain and in the United States into the mid-1950s, and very commendable stage performances were achieved at pressure ratios of up to 4/1. Following this period of development of the centrifugal compressor a growing preference in many aircraft gas turbine designs for the axial compressor with its higher efficiency and smaller frontal area (an argument recognised earlier by the German jet-engine designers) caused comparative neglect of the technology of the centrifugal compressor. It was not until the mid-1960s that the United States Army requirements for small engines for advanced helicopters resulted in a rapid revival of interest in the centrifugal's inherent advantages of stability of operation and high pressure ratio from a single stage, which, with sufficient research, might also be complemented with high efficiency, an essential improvement if usefully low specific fuel consumption was to be achieved. It was this impetus arising from the needs of the helicopter engine that gave birth to the current high levels of development and research which are being maintained in many parts of the world today. Britain has been no exception. It was undoubtedly the helicopter application which created renewed interest in the centrifugal compressor as is evidenced by the BS 360 engine, whilst the manufacturers of small gas turbines for other aeronautical applications (eg auxiliary power units, starter-generators, and remotely-piloted-vehicle propulsion) have also been directing attention towards the possibility of improving centrifugal compressor design technology.

Although the preceding paragraph has identified the small shaft-engine as being the first home of the centrifugal, it is worth noting that in the cores of some of the smaller by-pass thrust engines the centrifugal is also being utilised - in combination with axial stages upstream - because of its lesser vulnerability to losses associated with the very small dimensions of the high pressure turbomachinery.

Widening the field even further, the new technology of the centrifugal compressor for aeronautical application has inspired renewed efforts from designers of compressors for many other applications, for example, gas turbines for road vehicles, diesel engine turbochargers, chemical plant processes, large air conditioning plant, and factory workshop air supplies. A very thorough account of the historical development of the centrifugal compressor is given by Dean in Reference 1. Figure 1, which is reproduced from Dean's paper, shows how target pressure ratios have increased in recent years and the efficiencies with which they have been achieved.

In spite of the recent effort which has been directed towards improving the performance of the centrifugal compressor and towards the understanding of the flow within it, there still remain many difficulties in the design and comprehension of these machines. Assuming that these difficulties may be at least partially overcome by means of sufficient research, then there are further performance gains to be achieved. The bulk of this paper concentrates on what is known and also on what is not known concerning the sources of inefficiency and instability in the high pressure ratio centrifugal compressor (Section 2.0). This is followed by a discussion of the requirements of a modern compressor design procedure which uses the NGTE computer package as a

model, while the final section briefly outlines recommendations for future research necessities.

2.0 The sources of inefficiency in a high pressure ratio centrifugal compressor

2.1 Identifying the loss sources

It has naturally been a basic assumption in the preparation of this paper that the reader is familiar with the principle of operation of the centrifugal compressor. In an examination of the sources of inefficiencies of the compressor, however, it is usually helpful to remind oneself of the role of each component. Figure 2 illustrates the particular nomenclature of components chosen for this paper. Referring to this figure, the impeller imparts a stagnation enthalpy input to the air by increasing its angular momentum. The rise in stagnation enthalpy (in the absence of parasitic losses, to be mentioned later) is given by the Euler equation:

$$H_5 - H_3 = U_5 V_{w_5} - U_3 V_{w_3} \qquad \ldots.(1)$$

This stagnation enthalpy rise consists of both a static enthalpy rise and a dynamic head rise. The latter is so great (even though attempts to increase impeller diffusion may be made by the use of certain design features, as is discussed later) that further diffusion is required after the impeller in order that the energy increase of the air may be obtained in its most useful form, namely a static pressure rise. In a high pressure ratio compressor this can be achieved within a practicable diametral constraint only by the use of a vaned radial diffuser (Figure 2).

Between the impeller and the vaned diffuser it is necessary for both mechanical and aerodynamic reasons to have a vaneless space in which some intermediate diffusion takes place. Downstream of the vaned diffuser the flow is usually turned to the axial direction before entry to the combustion chamber by a radial-to-axial bend and a row of de-swirl stator vanes.

An additional component may be featured upstream of the impeller; should the impeller design result in the relative Mach number at impeller shroud entry being much in excess of unity it may be preferable, in order to avoid shock-associated losses (as is discussed later), to incorporate prewhirl vanes which impart to the air a tangential velocity component in the direction of rotation of the impeller (Figure 2) thus reducing the relative inlet velocity vector and hence Mach number.

Having recapitulated the terminology and functions of each component we can now proceed to identify and, approximately, to quantify the principal loss sources appearing in each component. Figure 3 presents a pictorial breakdown of the losses occurring within a compressor of 8/1 pressure ratio (designed within realistic aircraft gas turbine engine constraints) and was obtained using the computer program described in Reference 2. Outstanding in Figure 3 is the dominance of the impeller loss and it is because of this dominance that it heads the following Sections in which the losses in the major components are discussed in detail. Also discussed are the steps taken in recent years to understand and to reduce the losses.

2.2 Work input of the impeller

As was mentioned above the primary aim of the impeller is to give a work or enthalpy input to the airflow. As indicated by Equation (1), the useful work input depends only upon the blade speed at inlet and exit of the impeller and upon the absolute tangential velocity components at those stations. Blade speeds are limited only by impeller centrifugal stresses, the required tangential velocity component at inlet is easily obtained (and is frequently zero, ie zero prewhirl), which leaves only the exit tangential velocity component as a matter for some comment owing to the phenomenon of "slip". This term refers to the inability of the vanes to give perfect directional guidance to the fluid, an important effect especially at impeller exit where the relative flow angle is forced by slip to be greater than the vane angle (Figure 4). In an inviscid flow slip is present due to the relative rotation of a flow having a radial velocity component, while in a real flow the inviscid effect is augmented by the mixing of viscous boundary layers with the main flow as it leaves the impeller. Although slip is a complex phenomenon (as is evidenced by the many detailed treatments of the fluid mechanics, eg References 3, 4 and 5) the quantifying of its effect on the exit velocity triangle has largely been resolved, for practical purposes, by empirical or semi-empirical correlations of slip with the impeller design parameters on which it primarily depends, as described for example in References 3, 6 and 7, of which the last, due to Wiesner, is among the most widely used. Wiesner deduced that the increase in the tangential component of relative velocity V_{slip} is given by the simple correlation (referring to Figure 4):

$$\frac{V_{slip}}{U_5} = \frac{\sqrt{\cos \beta_{\infty_4}}}{Z^{0.7}} \qquad \ldots.(2)$$

Although the correlation from which this expression arose was subject to some scatter, it is to its credit that agreement between experimental and predicted work input such as that shown in Figure 5 can be obtained (see also Reference 2).

Thus an impeller may be designed with some certainty to give the required Euler stagnation enthalpy rise. The enthalpy rise is accompanied by a stagnation pressure rise whose magnitude depends upon the efficiency of the compression: the losses which reduce the efficiency and thus inhibit the pressure rise are discussed in the following Section.

2.3 Impeller losses

As was mentioned earlier considerable diffusion inevitably takes place within the impeller and thus appreciable frictional energy dissipation is incurred through the growth and possible separation of boundary layers subject to adverse pressure gradients on the many 'wetted' surfaces of the impeller. If boundary layer growth in the presence of the adverse pressure gradient were two-dimensional and the only source of loss, the impeller would be a comparatively easy machine to analyse and, relative to the reality, a highly efficient one. Unfortunately, the simple picture of boundary layer growth is complicated and, from the loss point of view worsened, by a number of additional factors, most of which are peculiar only to the centrifugal impeller (ie they are absent or relatively insignificant in, for example, the axial

compressor) and which are only very recently beginning to be understood as a result of widespread research effort. These additional loss-contributing factors will now be discussed under separate sub-headings:

Secondary flow

As in an axial compressor the rotating vanes of a centrifugal impeller produce the required increase in angular momentum of the airflow by means of a lift or static pressure difference Δp between the pressure surface (leading) and suction surface (trailing) as is pictorially represented in Figure 6. Temporarily confining the discussion to that part of the impeller flow which has little or no axial velocity component (ie flow which is mainly towards the impeller tip) for the sake of simplicity, we find by examining the tangential equilibrium of a fluid particle that the blade-to-blade static pressure gradient in fact provides the Coriolis acceleration of the particle,

$$\frac{1}{\rho r}\frac{\partial p}{\partial \theta} = 2\Omega W \qquad \ldots.(3)$$

For a particle somewhere near the mid-height of the channel (ie in the freestream remote from both hub and shroud boundary layers) Equation (3) is satisfied and the particle follows a radial path relative to the rotor. A particle within the hub or shroud boundary layers is subject to the same tangential pressure gradient as the freestream particle whilst having, however, a lower relative velocity W'. Thus, the otherwise radial relative motion of the particle is disturbed and the particle moves through its boundary layer towards the suction surface of the neighbouring vane (Figure 7) where it joins the suction surface boundary layer. There is thus continual transport of low momentum fluid from the hub and shroud boundary layers which feeds and thickens the suction surface boundary layer. The purely radial part of the impeller in which Equation (3) applies was chosen for illustration since the tangential momentum equation may be written in very simple form. Secondary flow occurs throughout the impeller, however, under the influence of a blade-to-blade static pressure gradient due to both Coriolis forces and the forces imposed by vane curvature. (Although secondary flows also occur in axial compressors their effect is less marked because of the shorter passage lengths and hence reduced opportunity for low momentum feeding.) Moore[8,9], in an excellent series of experiments at MIT, explored the flow within an isolated rotating radial channel and found that the suction side boundary layer was caused to thicken into a wake, the radial development of which is reproduced in Figure 8. Moore modelled the boundary layer growth and the feeding of the suction side layer by the hub and shroud boundary layers and, from the good agreement between theory and experiment, concluded that secondary flow accounted for the suction surface wake formation. There was little or no entrainment from the free-stream as shown by absence of reverse flow in the wake region (Figure 8). As Moore himself has commented, the concept of a thick suction side wake and a pressure side free-stream or jet was mentioned in the literature as early as 1923 (Reference 10) and in more recent years has been the subject of considerable theoretical attention by Dean and Senoo[11] and others. Lately Eckardt[12] using advanced instrumentation has observed the existence of the jet/wake pattern in a high speed centrifugal impeller. It will be clear that the effective blockage of the impeller exit limits the static pressure rise achieved by the impeller.

In spite of general acceptance of the growth of a thick suction surface wake in the impeller and in spite of the convincing evidence of Moore's work, there still exists considerable doubt that secondary flow is the only cause, or indeed the primary cause, of this flow pattern as the next Section will show.

Effects of rotation and streamline curvature on the turbulence structure of the boundary layers

Let us for simplicity consider the flow in a rotating, rectangular, radial-flow channel such as the one shown in Figure 9. The sketched distributions show how the relative velocity W and static pressure p are assumed to vary across the width of the channel. Outside the suction and pressure side boundary layers in the free-stream there is a tangential pressure gradient set up by the rotation of the channel as is represented by the following equation:

$$\frac{1}{\rho}\frac{\partial p}{\partial y} = 2\Omega W \qquad \ldots.(4)$$

Following the mechanism described by Moon[13] and by Johnston[14], a fluid particle in the suction side boundary layer momentarily displaced away from the wall without change of velocity will experience a tangential pressure force in a sense such that its movement away from the wall is discouraged. It may thus be said that the tangential pressure gradient has a stabilising influence on the suction surface boundary layer through discouraging the turbulent exchange of energy between the free-stream and the boundary layer. By similar arguments it may be shown that the reverse occurs on the pressure side where the boundary layer is de-stabilised by the pressure gradient. Thus it is argued that the suction surface boundary layer will thicken and possibly form into a wake with a Moore-type[9] profile, while the pressure surface boundary layer growth is inhibited, the whole once again supporting the experimentally observed jet/wake flow pattern.

This influence of rotation upon the boundary layer structure in radial rotating diffusers (ie impellers), which has been treated above in a simplified manner, has been the subject of considerable research by J P Johnston[14] and his colleagues at Stanford University[15,16]. Johnston has developed a generalised theoretical analysis which includes both the rotation effects and also the analogous effect of streamline curvature. To illustrate the latter, consider for example a curved, stationary channel (Figure 10). Here again a cross-channel pressure gradient exists, this time due to the curvature of the streamlines:

$$\frac{1}{\rho}\frac{\partial p}{\partial n} = \frac{V}{R} \qquad \ldots.(5)$$

By the same type of argument as was applied above to the effect of the rotational pressure gradient on the boundary layers, it can be shown that the convex side boundary layer in Figure 10 is stabilised (growth rate encouraged) whilst the concave side boundary layer is de-stabilised (ie growth rate discouraged).

While the simple geometries of Figures 9 and 10 serve to illustrate the principles, it is pertinent to note at this point how these two analogous effects may play important parts in determining the nature of the flow in an actual impeller. Figure 11a shows a blade channel of an impeller having radially stacked blades throughout and specifically having zero "sweep-back" ($\beta_{\infty_4} = 0$). Note the conditions of rotation and streamline curvature obtaining near the impeller exit: the vane suction surface is also a convex surface and thus is subject to the stabilising effects of both rotation and curvature while the reverse is true of the pressure surface since it is concave. It can be shown by considering simple examples that the rotational and curvature effects in a high pressure ratio impeller are of similar order of magnitude and therefore the absence or presence of either in a given impeller will be significant.

It is worth commenting that Figure 10 also applies to the meridional bend of the hub and shroud contours. Thus the worst 'convex' situation occurs at the corner of the shroud surface and the vane suction surface.

We have now discussed two possible suspects - secondary flow and turbulence structure effects - in the trail of evidence concerning the formation of the flow pattern in a rotating radial flow passage. The work of Rothe and Johnston[15] suggests that in the low aspect ratio passage of a centrifugal impeller both effects are important. It is clear that both are caused by the presence of the blade-to-blade pressure gradient. Since the Coriolis acceleration is the greater contributor to the pressure gradient and since the magnitude of the Coriolis accelerates increases towards the impeller tip, any method of off-setting the Coriolis contribution may help to reduce the consequent secondary flow and turbulence effects. Thus one of the three advantages of exit vane "sweep-back" comes to light. Figure 11b shows a sketch of an impeller having swept-back vanes - ie vanes leaning away from the direction of rotation. It is seen that the Coriolis acceleration is now opposed rather than reinforced by the acceleration due to streamline curvature, thus reducing the blade-to-blade pressure gradient near the impeller exit, and, it is thought, tending to inhibit the undesirable effects on the suction side boundary layer due to secondary flow and due to the rotational and curvature effects on turbulence structure. The widespread adoption of sweep-back in modern impeller designs has been in part due to these considerations although, as hinted above, this design feature has two further contributions and these are discussed in the later sections of this lecture. We shall now continue to examine further sources of loss within the impeller.

Losses at impeller inlet (inducer)

Losses can arise upstream of the inducer throat in three ways

a Boundary layer growth on vane and annulus walls due to diffusion (at zero incidence).

b Increase of vane surface diffusion rates due to incidence.

and c Shocks.

It is convenient to think in terms of these separate components although the actual loss-producing process in a high speed impeller will in fact be a complex combination of all three. Temporarily imagining that the losses due

to b and c are negligible (ie both inlet relative Mach number and incidence are small), subsonic diffusion and boundary layer growth would occur upstream of the throat, the amount depending on how much change in vane camber angle occurs ahead of the throat. Progressing to the case where the approach Mach number is in fact in excess of unity, a bow shock will occur ahead of the vane leading edge (Figure 12a). The shock will result in a direct stagnation pressure loss in the free-stream but this will be small (eg, from shock tables, 1 per cent stagnation pressure loss for a pre-shock free-stream Mach number of 1.2). More serious may be the effect of the shock on the already growing boundary layers which, on encountering the sudden pressure rise will thicken and, if the shock is strong enough, may separate. It is also to be noted that if the vane camber angle is reducing ahead of the shock where the flow is supersonic, acceleration will occur and the shock when it comes will be stronger still.

If, additionally, there is positive incidence a leading edge separation may occur. In this case supersonic expansion takes place around the separation bubble. Even though re-attachment may follow, the suction surface Mach number will have been increased, thus leading to a stronger shock (Figure 12). In the presence of negative incidence an oblique shock will occur at the leading edge.

In a high pressure ratio machine it is possible for all these effects to be present at once. Positive incidence at supersonic approach Mach numbers will result in additional net supersonic acceleration as the flow rounds the leading edge[17] on to the suction surface of the vane, thereby increasing the strength of the terminal shock. These loss sources are known to exist in the inducer but the calculation of the increase of boundary layer thickness through the shock is not yet possible, though much has been done towards the study of this subject in connection with isolated aerofoils[18]. Relatively simple models have been proposed for the effects of a and b in subsonic flow, one of which is contained in the performance prediction program described in Reference 2.

Having briefly described the inducer losses, we must conclude that the estimation of their contribution towards the total impeller loss must at present be chiefly qualitative. However, there is sufficient evidence from axial transonic fan experience to suggest that where an impeller design requires that the approach Mach number is greater than or equal to say 1.2 steps should be taken to counter the potential problems. Before examining what measures may be taken, let us first look at the conditions under which high inducer Mach numbers may arise.

Figure 13, taken from Reference 19, shows the variation of inducer shroud approach Mach number for varying stage pressure ratio and pre-whirl angle for a constant value of specific speed, N_S. (The parameter specific speed is fully defined in the Notation (p25) and represents the ratio of impeller mass flow rate to "wetted area", a high value of N_S implying a high value of this ratio. For low Mach number impellers Balje's classic impeller loss study[20] indicated that there exists an optimum value of N_S ($\simeq$100) at which the impeller efficiency is maximised.) Referring to Figure 13, it may be seen that inlet relative Mach number increases rapidly with pressure ratio, a value of about 1.5 being reached at a pressure ratio of 10 if the pre-whirl is zero. It may also be observed that increase of pre-whirl angle reduces the approach Mach number and the reason for this is apparent from the velocity triangle

shown in Figure 2. Thus one possible solution of the Mach number problem appears, but it is not without drawbacks. The pre-whirl vanes will incur a loss of their own but this is very small (see Figure 2). More important are the added weight and complexity due to the presence of the vanes themselves and the additional impeller vane and disc stresses arising from the increased tip speed which is required to compensate for the pre-whirl angular momentum deficit. (Equation (1).) Increased diffuser approach Mach number with consequent increase in diffuser loss (see later) also follows from the increased tip speed.

A second method of attacking the Mach number problem is to reduce specific speed below the Baljé 'optimum' as is illustrated in Figure 14 (also taken from Reference 19) the intention being that the reduction of shock-associated losses should outweigh the increase of low-specific-speed-associated losses (increased "wetted" area). Calculations of the opposing losses are not sufficiently good at present for an optimal choice to be made. It should be noted that, in a gas turbine application, the designer is in any case forced to select a value of specific speed of a high pressure ratio centrifugal impeller which is well below the 'optimum' because of stress limitations on the driving turbine. The physical disadvantage of a low specific speed impeller is its larger tip diameter and hence larger frontal area and weight.

In concluding this section on inducer losses, it will have become clear that, for the two methods of reducing the losses that have been described, our theoretical knowledge is at present too poor to permit an optimum choice of pre-whirl and specific speed to be made without resort to experiment or development. Well-controlled comparative impeller tests in which only the parameter of interest is varied are extremely difficult to set up because of the many parametric interrelationships which exist. What experimental evidence there is tends to be random and not entirely conclusive. However, for illustrative purposes two items are worth mentioning. Firstly, at the Rolls-Royce Helicopter Engine Group (ex-Small Engine Division) tests of a 5/1 pressure ratio high specific speed impeller[21] were conducted with and without pre-whirl. In the tests without pre-whirl the shroud inlet relative Mach number was 1.25; with the addition of 20° of pre-whirl the Mach number dropped to 1.1. Somewhat surprisingly, and in contradiction to the predictions of the best available efforts at loss prediction , there was no difference in stage efficiency at the design pressure ratio. It is possible, but not very probable, that differences in matching of the diffusers could have spoilt the comparison.

As a somewhat subjective illustration of the possible benefits of low specific speed, an impeller-alone calibration recently carried out at the NGTE on a zero pre-whirl compressor designed for PR = $6\frac{1}{2}$ and N_S = 68 (a very low specific speed resulting in an inducer Mach number of just less than unity) has indicated impeller efficiency levels which could well be competitive with the alternative design philosophy of higher specific speed in conjunction with pre-whirl. This compressor is discussed again in Section 3.2.

Effect of impeller velocity ratio

The preceding sections have drawn a picture of the impeller flow as one which is dominated by thick boundary layers whose growth is in general augmented by incidence, shocks, secondary flow, and boundary layer turbulence suppression. Even in the absence of these effects, substantial boundary layer

growth would of course take place, encouraged by the adverse pressure gradient. A parameter which usefully describes the overall impeller diffusion is the relative velocity ratio, VR:

$$VR = \frac{W_5}{W_{3\,shr}}$$

(It should be noted that W_5 is the tip relative velocity assuming instantaneous mixing of boundary layers with core or free-stream. The shroud entry velocity $W_{3\,shr}$ is used in the denominator in preference to the hub or mean value, since in most impeller designs $W_{3\,shr} > W_{3\,hub}$, implying greatest diffusion along the shroud.) In the absence of boundary layer separation, the resultant effect of boundary layer growth on the one hand and of the mixing of boundary layers with the free-stream on the other indicate that VR should be minimised (for a given inlet velocity) for maximum impeller efficiency. Figure 15, which shows the results of calculations of impeller efficiency for varying VR performed using the program of Reference 2, illustrates the point. Unfortunately, it is certain that the reality is more complicated. The separation that would in any case occur due to large local pressure gradients is certainly precipitated earlier on the suction surface by the effects which encourage wake formation as described earlier. There is thus a limit on the amount of diffusion (ie the value of VR) which the impeller will stand, and it is almost certain that there is in fact an optimum value of VR as suggested in Figure 15, although the value of the optimum will be strongly related to other design parameters (eg blade loading parameters, Mach number level etc). As yet there is no evidence on which to base estimates of optimum VR. Comparative experiments on actual impellers are extremely difficult to set up without the comparison being spoilt by other parameters changing as well. The development, for actual impeller calculations, of boundary layer methods such as Moore's[8] which attempt to account for the factors affecting wake formation may enable the optima to be estimated theoretically. Values of VR currently in use range from about 0.5 to about 0.8.

2.4 The diffuser

Under this heading we shall cover both the vaneless space and the vaned diffuser. The vaned diffuser has three primary requirements:-

1 To convert as much of the inlet kinetic energy as possible into static pressure.

2 To achieve this within as small a radial distance as possible to comply with engine overall radius limitations.

3 To have its throat area correctly matched to the impeller exit conditions.

Covering requirement 1 first, we find that the diffusing ability may be conveniently described by two parameters. The first is the ideal pressure recovery coefficient:

$$C_{p\,ideal} = \frac{\text{rise in static pressure between throat and exit}}{\text{throat dynamic head}}$$

assuming an isentropic diffusion. $C_{p_{ideal}}$ is a function only of the area ratio of the diffuser and the throat Mach number, as is shown in Figure 17, and represents the potential diffusing capability of the diffuser. The second parameter is the actual pressure recovery coefficient C_p (ie as defined above but with irreversibility) and the value of this parameter, or if preferred, the ratio $C_p/C_{p_{ideal}}$, is a measure of the efficiency of the diffuser, ie how much of the potential diffusing capability the designer has made use of by the minimisation of losses.

The losses within the diffuser channel naturally depend upon the behaviour of the boundary layers on the channel walls. Their behaviour, it transpires, can vary between very marked extremes. Fox and Kline[22] usefully classified the flow within two-dimensional diffusers into regimes which are best expressed on a map whose axes are the length/width ratio (ℓ/w) and the area ratio (AR) which together fix the divergence angle of the channel (Figures 17 and 18). It is qualitatively clear from Figure 17 that pressure recovery must vary a great deal over the map, but exactly what is its variation and on what other parameters if any does this variation depend? A creditable method of calculation of the unstalled recovery of two-dimensional, straight walled, subsonic diffusers was developed by Reneau et al[23] by solving the momentum and continuity equations of the boundary layer. Their method lacked a separation criterion, however, and Cocanower, Kline and Johnston[24] produced a similar calculation method which included a separation criterion and also extended coverage of the geometry to conical, annular, and three-dimensional diffusers. Comparison with measurements was impressive, but Runstadler and Dean[25], recognising the need for high Mach number data for diffuser design for high pressure ratio centrifugal compressors, produced a vast experimental data contribution which is probably the most widely used source of diffuser design information.

Using a straight centre-line, isolated, diffusing channel, Runstadler systematically varied the values of the five parameters which he considered to be the most influential (throat blockage, length/width ratio, area ratio, throat Mach number and throat aspect ratio) - and measured pressure recovery for large ranges of these parameters, the result of which is an extremely useful set of performance graphs expressed in terms of C_p. Runstadler found that of the five parameters tested the most significant were the throat blockage, the length/width ratio (ℓ/w) and the area ratio (AR), the last two of which fix the divergence angle of the channel as stated above. For fixed values of throat blockage, aspect ratio and Mach number, a typical Runstadler performance graph is as given in Figure 19 where C_p is expressed as a function of ℓ/w and AR on the type of map proposed by Fox and Kline. It may be seen that the graph exhibits both a ridge of high recovery (following divergence angles between 6 and 8 degrees) and the beginnings of a peak towards the top right-hand corner.

Clearly the designer would like to aim for peak recovery but if he did so the large ℓ/w involved might easily contravene engine-imposed radial constraints, which was one of the three primary considerations mentioned at the beginning of this Section. Possibly the best choice of positioning on the Runstadler plot is the tangency point of the line of maximum permissible ℓ/w and a C_p contour (Figure 20). This maximises C_p for a fixed radial limitation on the diffuser and for fixed (near unity) aspect ratio. Factors affecting the selection of the inner radius of the diffuser are discussed later.

The reader should not be left with the impression that the Runstadler data provide a perfect method of diffuser geometry selection and a faultlessly correct value of pressure recovery coefficient for a chosen geometry. The accuracy of the C_p contours is hampered in the real stage design by doubt about the value of the channel throat blockage (although quite promising "one-dimensional" methods of blockage growth calculation through vaneless space and semi-vaneless space are now available eg Reference 2) and also by the effect of unsteady and circumferentially non-uniform flow which the diffuser channels receive from the impeller. The latter effect almost certainly reduces the diffuser recovery and may also promote surge. No theory exists for the treatment of the unsteady approach flow.

As a means of increasing the C_p obtainable within given radial limits some designers have used mild inward centre-line curvature so that ℓ/w may be increased. Very significant gains are probably prohibited however, since the gains in ℓ/w produced by high centre-line inward curvature will be partially offset by increasing secondary losses arising from the effect of streamline curvature on the wall boundary layers[26]. Thus curved diffuser channels will have C_p values lower than those given by Runstadler for straight channels having other parameters the same.

We shall now consider the losses arising in the vaneless space and semi-vaneless space and go on to discuss how consideration of the losses may affect the choice of diffuser inner radius. As was described in Section 2.2 the impeller develops a very non-uniform flow profile at exit. Most theoretical models of the vaneless space flow assume that the non-uniform impeller exit flow mixes out instantaneously to a uniform flow, whilst Eckardt's experimental observations[12] show that actual mixing is much less rapid. In any case, on the walls of the vaneless diffuser new boundary layers will begin to grow and appreciable blockage may be incurred up to the diffuser leading edge station (eg a typical blockage of 5 per cent could grow within a radius increase of 5 per cent, even assuming rapid mixing of the impeller flow). Remembering that, according to the Runstadler plots, throat blockage has a strongly undesirable effect on C_p, it could appear that vaneless space boundary layer growth should be minimised by reduction of the extent of the vaneless space. Two factors limit such a move, however. Firstly, close proximity of impeller and diffuser vanes has been known to cause excessive vibrational excitation of the impeller vanes leading to subsequent fatigue failure of the impeller. Secondly, since impeller absolute exit Mach numbers above unity are encountered for pressure ratios in excess of about 4, the designer may wish to take advantage of the shock-free transition to subsonic flow which is provided by an extended vaneless space, with the intention of eliminating shock-associated losses and blockage increase in the vaned diffuser pre-throat region (or semi-vaneless space). There are thus two philosophies applying to the selection of vaned diffuser inner radius (as illustrated in Figure 21).

1 Short vaneless space and low blockage growth coupled with high vane diffuser approach Mach number and relatively rapid blockage growth across the shock.

2 Longer vaneless space and consequently greater boundary layer growth, but resulting in subsonic approach Mach number.

The first philosophy has the advantage of either higher channel pressure recovery if the outer radius is fixed (due to larger ℓ/w) or of reduced outer radius (as shown in Figure 21); in the latter philosophy the throat Mach number may be lower anyway so that good channel recovery is not so vital.

In their efforts to overcome the many obstacles to good recovery of conventional radial diffusers, some designers have been forced to look to the unconventional solution, for example:

i the pipe diffuser[27] developed by United Aircraft of Canada in which vanes and channels are replaced by discrete drillings or pipes lying with their axes tangential to the impeller tip circle in the plane of the vaneless space (Figure 22). The pipe diffuser has resulted in significant improvements in stage efficiency operating in transonic approach flow; it is said to be less sensitive to high Mach numbers, high inlet blockage and circumferentially distorted flow. It also offers ease and economy of manufacture.

ii the free-rotating vaneless diffuser tested by Rodgers et al[28] of Solar in which the hub-side of the vaneless diffuser forms part of an independently rotating disc, concentric with the impeller, and driven by the drag of the air flowing across its surfaces (Figure 23). Loss in the vaneless space is reduced by virtue of the reduced relative velocity. The success of the rig trials in improving pressure recovery of the total diffusing system (including a vaned diffuser) tends to be marred by the inevitable mechanical complexity.

iii the tandem diffuser investigated by Pampreen[29] in which two rows of aerofoil vanes were demonstrated to give improved surge margin and slightly improved efficiency when operating between the same radial limits as a single-row diffuser. The improvement is brought about by discontinuous boundary layer growth from inlet to exit. The only disadvantages appear to be the slightly greater complexity and cost of manufacture, and the relative scarcity of design data.

2.5 Surge

In preparing a paper on high pressure ratio centrifugal compressors one feels obliged to include a discussion on surge. Unfortunately since ignorance still far outweighs knowledge in this topic such a discussion is no easy matter.

Comparative tests of the same impeller with both a vaneless diffuser and a vaned diffuser invariably result in a smaller surge margin in the vaned diffuser test (eg Figure 24). The implication is that the vaned diffuser, if present, is the surge-controlling component in a compressor stage. Jansen[30] has made a theoretical study of the mechanism of stall in long vaneless diffusers. He attributes stall in this case to the occurrence of inward radial flow in the wall boundary layers due to imbalance between the radial pressure gradient and the tangential velocity of the low momentum fluid in the boundary layer (ie secondary flow). It is conceivable that the same type of flow breakdown occurs in the vaneless space when a vaned diffuser is present, an earlier stall being caused by the more severe pressure gradients brought about by the presence of the vanes themselves (eg Figure 26). Amann et al[31] have suggested that the circumferentially non-uniform radial pressure gradient caused by the

presence of the diffuser vanes causes periodic reversal of flow in the vaneless space, mainly in the shroud boundary layer. The backflow intermittently re-entering the impeller causes a type of rotating stall which finally results in the low frequency system unsteadiness associated with surge. The hypothesis is partly reinforced by hot-wire measurements in the vaneless space. Kenny[32] also considers that the vaneless space plays an important role in the promotion of stall, but his reasoning is altogether different. Rightly recognising the diffuser throat blockage as having an important effect on the stability of the channel boundary layers, he asserts that the pressure rise from impeller tip to diffuser throat will increase the blockage as the tip-to-throat diffusion rises with falling mass flow, the process eventually resulting in separation and loss of recovery in the diffuser channel. Figure 26 (taken from Reference 32) shows the experimental evidence. The scatter around the recommended level of pressure rise parameter (0.45) is large, however, and trials of Kenny's criterion on other data produce even wider discrepancies. This does not necessarily mean that the proposed model of stall is wrong. It could simply mean that other aerodynamic or geometric features, of which the unsteady and circumferentially non-uniform flow around the impeller may be among the most likely contenders, are also important. The same qualification applies to other mechanisms and criteria which have recently been tested with only limited success in the course of the development of the NGTE off-design performance prediction program[2]. These include: Mach number ratio between diffuser approach and throat; blockage ratio between the same stations; and diffuser incidence. The incentive to involve a parameter dependent upon diffusion up to the throat is strong, since small adjustments to diffuser throat area have been shown experimentally to influence stage surge mass-flow (as well as stage choke-flow).

The text-book explanation of surge of any type of compressor (eg Dean[33]) suggests that surge occurs at the peak of the pressure ratio/mass flow characteristic, the positive gradient part of the curve defining the unstable operating region of the compressor. This explanation, even if true, adds nothing to the state of knowledge concerning the initial stall that leads to the stage instability. Centrifugal compressor stage performance characteristics sometimes give support to the "peak pressure rise" criterion but the evidence does not appear to be strong enough to enable this feature to be used as a surge criterion in, for example, the prediction of performance characteristics. The very flat characteristics of zero sweepback impellers, in particular, would provide a very challenging test for such a criterion.

The brief discussion above concerning the slope of the pressure rise characteristic leads us to one of the better accepted methods of improving surge margin, namely, impeller vane sweepback. By virtue of the shape of the tip velocity triangles it happens that reduction of mass flow increases the work input and hence pressure rise of a sweptback impeller (Figure 27), whilst in a radial outflow impeller there is little effect of flow reduction on work input. Thus the work input and pressure ratio characteristics of the former tend to feature stepper negative slopes than those of the latter, so delaying to a lower mass flow the position of peak pressure rise and, according to the earlier argument, surge.

In addition to the effect on the slope of the characteristic, sweepback also reduces the absolute Mach number at impeller tip (Figure 27) and hence also the Mach number at diffuser approach. Not only could this be a further factor in delaying surge (if any of the "diffusion-up-to-diffuser-throat-

mechanisms" are believed), but it may also be a contribution towards reducing diffuser loss and hence improving stage efficiency.

Amann et al[31] took more unorthodox steps to improve surge margin. Directed by his hypothesis of the mechanism of vaneless space periodic stall described earlier in this Section, he reasoned that, if the lower momentum fluid leaving the impeller (the wake) when confronted with a peak in the diffuser vane pressure gradient field, could be allowed circumferential communication with a trough in that field, the fluid which otherwise would be turned back into the rotor might flow circumferentially via the communicating flow path. Amann tested the theory on a 4/1 pressure ratio compressor in which the communicating flow path took the form of a slot and a chamber as shown in Figure 28. The surge margin was indeed improved as is shown in Figure 29.

Another type of circumferential communication which has apparently resulted in improvements in both efficiency and surge has been patented by United Aircraft of Canada. Figure 30 shows the arrangement of a succession of circumferential slots in the shroud casing of the impeller and the result on performance is shown in Figure 31. The mechanism would appear to be based on the reduction of secondary flow feeding of the wake by the effective removal of the blade-to-blade pressure gradient at the shroud.

In conclusion, very significant success in improvements of surge margin must now depend upon a better understanding of the mechanism of stall and surge.

3.0 The requirements of a centrifugal compressor design system

This section begins by summarising the essential requirements of a system for the design of high performance, high pressure ratio, centrifugal compressors. Every group or organisation active in this field today will have developed or adopted the constituent parts of such a design procedure although clearly the exact form and degree of sophistication of these tools will vary from one organisation to another. We shall then continue by using the NGTE Impeller Computer Design Package (ICDP) as a means of describing the more detailed use of modern design methods, and finally present briefly the design and test results of a centrifugal compressor which has recently been designed using the ICDP.

The essential requirements of a centrifugal compressor design system may be summarised as follows:

1 Preliminary design procedure for impeller and diffuser (with means of off-design performance prediction, if possible).

2 Impeller vane geometry definition procedure.

3 Aerodynamic analysis of impeller flow.

4 Impeller stress analysis.

5 Impeller manufacturing procedure.

3.1 The NGTE Design System

3.1.1 Preliminary design

Requirement 1 (the preliminary design procedure) is, in the case of the NGTE Design System, met by a computer program[34] which will, upon the provision of a number of parameters that describe the required duty of the machine, calculate sufficient parameters for the overall impeller geometry to be defined. The program solves the "one-dimensional" equations describing the work input, continuity, and velocity triangles. Figure 32 schematically represents this preliminary design program with its input and output. There are many possible forms in which this calculation may be arranged with some of the dependent variables exchanged for some of the independent variables, but the particular arrangement shown has proved to be an extremely useful tool in the initial stage of examining a large number of candidate compressor designs.

Having obtained in this way the dimensions and flow conditions at impeller inlet and exit it is then possible to solve the two-dimensional boundary layer equations in the vaneless space, as implemented in the computer program of Reference 2, to obtain diffuser approach conditions including boundary layer blockage at any radial station (for example, a radial station chosen on the basis of diffusion to a pre-specified level of Mach number). Knowing the approach conditions, the channel diffuser throat area may be selected and, with the additional specification of diffuser vane number and exit radius, the diffuser channel geometry may be defined, its length/width ratio and area ratio being optimised by reference to the Runstadler data[25], which also of course provides an estimate of the pressure recovery of the final choice of channel geometry.

The "one-dimensional" flow path geometry (ie diameters, annulus heights, throat areas and inlet and exit vane angles) may thus be established. The performance prediction program may now be used to conduct a design point and off-design analysis of the selected one-dimensional geometry. At the design point this calculation will merely serve as a check on the work accomplished using the preliminary design program, but extra information at off-design conditions such as inducer choking flow may be computed. If desired, a complete set of compressor characteristics may be predicted. So far, however, no satisfactory means of predicting the surge line has been found.

3.1.2 Impeller vane geometry definition procedure

The impeller design has reached the stage as described in the last section where only the inlet and outlet geometry has been defined. It is now necessary to clothe the impeller with a hub and shroud meridional shape, vane camber angle distribution, and a vane thickness distribution. Traditional methods of geometry definition have employed relatively simple shapes (eg circular arcs and straight lines) for the specification of hub, shroud, and vane camber distribution, usually described on a manufacturing drawing. These methods have proved satisfactory for the representation of impeller vanes which were radially stacked, but the requirement to design vanes which were non-radial (eg backward swept at outlet) resulted in the development of a new technique at NGTE (Requirement 2).

The essence of the new technique is to describe the impeller geometry precisely by analytic surfaces. An initial skeleton, defined by the impeller axial length and tip width, and by the inlet and exit diameters and vane angles, is clothed with three analytic surfaces (camber surface, pressure surface and suction surface) which then entirely define the impeller shape (see Figure 33). The mathematical details of the technique are given in Reference 35. This method of geometry representation has been arranged for use on a graphical storage tube terminal working in an interactive mode with a time-sharing computer. By virtue of the analytic nature of the vane geometry modelling system it is relatively easy to compute and display immediately graphical (or numerical) distributions of the parameters of interest. Figures 34 and 35 for example show a computer-generated distribution of camber angle and views of the inducer channel shape, respectively. Figure 36 shows two perspective views of a computer-defined outline geometry of a sweptback impeller - a "frill" which becomes surprisingly useful in a system where the manufacturing drawing has no part to play. There are a number of additional benefits which stem from the analytic nature of the geometry model and since these benefits are directly related to the requirements 3 to 5 mentioned above they will be described in the following Sections in conjunction with the method chosen to satisfy those requirements. It is, of course, vital that the shape of the impeller channel should be selected such that the efficiency loss, as far as the designer can predict, is minimised. The next section therefore describes the methods used for analysis of the impeller flow.

3.1.3 Aerodynamic analysis of impeller flow

Section 2.0 will have given the reader an appreciation of the complexity of the flow within the impeller passages. Unlike the flow in axial turbomachines, which may with some optimism be analysed with potential flow methods, the flow in a centrifugal impeller apparently exhibits such strong three-dimensional effects, and such large boundary layers (which become towards exit as prominent as the free stream itself) that there would appear at first sight to be little point in attempting to apply potential flow analysis to such a daunting situation. These are the considerations which have led Dean to reject the notion of using ideal flow solutions[1]. This argument is, however, halted abruptly when one discovers that there is as yet no practicable alternative. As far as is known all impeller flow analysis methods in use today are based on the solution of the inviscid flow equations although certain refinements have been introduced to a greater or lesser degree in attempts to simulate the most significant of the centrifugal impeller's flow peculiarities. As is well-known, the two-dimensional turbomachinery potential flow equations as expressed by Wu[36] are written in two stream surfaces - a hub-to-shroud, or S2, mean-stream-surface in which the flow is assumed to be axisymmetric, and a blade-to-blade or S1 stream-surface which requires a previous S2 solution for full definition of the surface geometry. Both problems have traditionally been solved by one of two methods - the matrix approach or the streamline curvature solution.

While attempts to predict the blade-to-blade flow continue to be worth pursuing (eg References 37 and 38), at NGTE, although an investigation of the applicability of a blade-to-blade solution[39] to the impeller problem has been made, it has been concluded that the best and quickest practicable approach is to obtain only a hub-to-shroud mean-stream-surface solution whilst the conditions obtaining at impeller vane surfaces are calculated only approximately from a knowledge of the mean-stream-surface velocity vector and either angular

momentum or absolute circulation considerations. The particular program in use in the ICDP is the matrix through-flow program originally written by Marsh[40] and recently modified for use in centrifugal impellers[41]. The modifications, which are relatively crude, are as follows:

1 Redistribution of mean-stream-surface camber angle towards the radial portion of the impeller in order to simulate the effect of slip.

2 Allowance for simulation of boundary layer blockage (calculated or estimated external to the program) to be incorporated on hub, shroud, and vane surfaces; the unblocked flow is isentropic.

3 The ability to cater for intervanes in the calculation of vane surface flow conditions.

An an alternative to 2, which is essentially a crude model of Eckardt's observed flow or Dean's postulated model, the blockage can be ignored and the impeller inefficiencies simulated by a distribution of polytropic efficiency. More refined throughflow impeller calculations attempt to incorporate boundary layer development within the iterations of the potential flow solution.

The geometric data preparation for this program is formidable but thanks to the analytic geometry model it has been possible to arrange automatic data preparation via an appropriate interface program.

The mean-stream-surface and vane surface velocity distributions for a particular trial impeller geometry can thus be obtained from the matrix through-flow program. These must then be assessed and, if considered unsuitable, appropriate revisions may be rapidly made to the trial impeller geometry and the aerodynamic analysis repeated. In the absence of an in-built boundary layer calculation the criteria at present used to assess the predicted velocity distributions are:

1 Minimisation of pressure gradients (for avoidance of two-dimensional boundary layer separation).

2 Avoidance of peaks in the distribution of blade-to-blade pressure difference (in order to minimise secondary flow and rotational/streamline curvature effects on boundary layer stability).

3 Avoidance of near-zero velocity on pressure surface.

The predicted blade surface relative velocities have been found to be unreliable upstream of the throat (because of unavoidable discontinuities in the specified mean-stream-surface geometry at the leading edge) and near the trailing edge where, owing to the approximate nature of this part of the calculation, the aerodynamic vane loading does not fall to zero. Examples of the use of these flow predictions in the design of an impeller are discussed in Section 3.2.

3.1.4 Impeller stress analysis

The method of stress analysis chosen to meet requirement 4 is a three-dimensional finite element program[42] which is a modified version of an original program[41] obtained from Swansea University. As with the aerodynamic analysis, complex geometric data are required, but with the use of a further data interface program, also described in Reference 42, the transformation from the analytic surface description becomes relatively easy.

3.1.5 Impeller manufacturing procedure

The capability for in-house manufacture of impellers (requirement 5) was achieved by the addition of two cam-controlled rotational and tipping axes to an existing 3-axis, numerically controlled, milling-machine. The complicated calculation of the numerical data required to define the path of the cutting tool is performed by a computer program which once again is able to draw upon the precise vane description of the impeller geometry.

3.2 Use of the Impeller Computer Design Package for the design and manufacture of a research impeller

Prior to the introduction of the ICDP work had been commenced on the design and manufacture of a compressor of $6\frac{1}{2}/1$ pressure ratio, this being a duty which was considered to be relevant to small engines for aircraft application. Other design parameters for this compressor (to be known as Compressor 'A') are as follows:

Specific speed (Baljé definition) - 68

Rotational speed - 40,000 rev/min

Mass flow - 1.82 kg/s

Design overall stage efficiency - 0.80

Design impeller efficiency - 0.90

The test characteristics obtained from the final build of Compressor 'A' are shown in Figure 37. An overall isentropic efficiency of 79 per cent was achieved at a pressure ratio of $3\frac{1}{2}$, falling to 75 per cent at the peak pressure ratio of 5.9. Good flow margins (choke-to-surge) were obtained at all rotational speeds covered by the tests. The shortfall in peak pressure ratio at the design speed is found to correspond almost exactly to that in efficiency, the assumed and measured slip factors being in very close agreement. Figure 38 shows the test characteristics obtained from a test of the impeller alone, the efficiency and pressure ratio being measured at a station close to the impeller tip. It will be seen that the impeller efficiency has been largely responsible for the low stage efficiency. Choke flow is uncomfortably close to design flow. Following the completion of the ICDP, the impeller of Compressor 'A' was analysed with the modified matrix through-flow program. An illuminating sample of the results of this analysis is shown in Figure 39 which presents the variation of blade-to-blade pressure difference plotted against meridional arc length through the impeller for both hub and shroud stations. It is clear that high vane loadings exist in the inducer and these may have caused unnecessarily early formation of a suction surface wake.

The first impeller to be designed using the ICDP (and known as Impeller 'B') was selected to have the same design point in every respect as its predecessor, Impeller 'A', but the vane camber distribution and annulus shape were to be designed from the outset with the guidance of the through-flow analysis. The vane sweepback angle was chosen to be 30°, to give good stability of operation. Figure 39 compares Impellers 'A' and 'B' in terms of their meridional view and distribution of the vane camber angle whilst Figure 40 compares the predicted blade-to-blade aerodynamic loading distribution for both impellers. It is clear that the loadings of Impeller 'B' are much reduced compared with those of Impeller 'A'. These predicted improvements are supported by the experimental observations. The impeller-alone calibration shows clear improvements over Impeller 'A' in terms of both efficiency and flow margin as is shown from a comparison of Figure 41 with Figure 38. A stage test is to follow. It is hoped that the apparent improvement in impeller performance will be maintained in the stage calibration.

4.0 Future research in centrifugal compressors

The centrifugal compressor offers a relatively inexpensive, simple, and robust means of obtaining high pressure ratio and good flow range from a single compression stage in gas turbine engines of up to about 2000 shp output. Present stage pressure ratios in current production engines are limited to about 8 because at higher pressure ratios the efficiency and surge margin become unacceptable. In order that stage pressure ratios may be increased, thus offering less dependence upon boosting from LP axial stages and therefore even greater simplicity and cheapness, means must be found of reducing the losses which have been the principal subject of this paper. There would be a natural "spin-off" to the lower pressure ratio duties. It appears that the most promising paths of research to meet this need should include the following:

1 Further experimental investigation of the impeller flow,

a in high speed, high pressure ratio machines using fast response instrumentation such as laser anemometry and piezo-electric or strain-gauge-type static pressure probes, the forerunner of which is the work of Eckardt[12] at DFVLR.

b in low speed impellers whose scale is sufficiently large that measurements of boundary layer development may be made.

2 Development of the impeller flow models for application in the real impeller environment, with the use of data gained from 1. The most likely path seems to lie through boundary layer methods such as Moore's[9].

3 The design of efficient transonic diffusers (approach Mach number > 1.2).

4 Efficient diffusers of smaller radial extent (possibly using boundary layer suction).

5 Understanding of the effects of unsteady approach flow on diffuser recovery and surge.

6 Understanding of the causes of stage-stall and surge and further development of means of delaying surge (eg labyrinths, slots etc).

7 The equalisation of diffusing duty between shroud and hub.

8 The design of efficient transonic inducers ($M_{s_{shr}} > 1.3$) including 'separate inducers' or 'tandem inducers'
and
(the alternative solution to the high inlet Mach number problem).

9 The investigation of stage performance with very low specific speed ($N_S < 65$) and high pressure ratio (PR > 8).

Acknowledgements

British Crown Copyright, reproduced by permission of the Controller, Her Majesty's Stationery Office.

The author is grateful to Dr. M. V. Herbert whose suggestions and advice in the preparation of this paper were most valuable.

Notation

AR	diffuser area ratio (Figure 19)
C_p	diffuser pressure recovery coefficient (see text, Section 2.4)
$C_{p_{ideal}}$	ideal recovery coefficient (see text, Section 2.5)
H	stagnation enthalpy
ℓ	diffuser channel centre-line length (Figure 19)
M	Mach number
n	co-ordinate direction perpendicular to streamline
N_s	specific speed $\left\{ \dfrac{\text{rotational speed} \times \text{vol flow}^{\frac{1}{2}}}{\Delta H_{isen}^{\frac{3}{4}}} \right\}$
	where rotational speed is in rev/min
	vol. flow is in ft^3/s
	ΔH_{isen} is in ft
p	static pressure
PR	stagnation pressure ratio
Q	mass flow
r	radius (from compressor axis)
R	radius of curvature of streamline
U	blade speed
V	absolute velocity
V_{slip}	tangential velocity deficit due to slip
VR	impeller relative velocity ratio $\dfrac{W_5}{W_{3\,shr}}$
w	diffuser throat width
y	co-ordinate direction from blade-to-blade of rectangular channel
Z	vane number
α	absolute air angle (relative to meridional direction)

β_∞	vane camber angle (relative to meridional direction)
θ	cylindrical co-ordinate
ρ	density
Ω	angular velocity

Subscripts

1	Upstream of prewhirl vanes	see Figure 2
2	Downstream of prewhirl vanes	
3	Inducer approach	
4	Impeller tip (pre-mixing)	
5	Impeller tip (post-mixing)	
6	Diffuser approach	
7	Diffuser exit	
shr	shroud	
hub	hub	
w	tangential component	
r	radial component	
isen	isentropic	

Superscript

'	relative to impeller

REFERENCES

No	Author(s)	Title, etc
1	R C Dean, Jr	The centrifugal compressor Creare Inc Technical Note No TN-183, 1973 Also Gas Turbine International, March-April and May-June, 1973
2	M V Herbert	A method of performance prediction for centrifugal compressors NGTE work to be published
3	J D Stanitz	Some theoretical aerodynamic investigations of impellers in radial-and mixed-flow centrifugal compressors ASME Paper No 51-F-13, 1951
4	Sh Yedidiah	New look at the slip in a centrifugal impeller Proc Inst Mech Engrs, Vol 188, pp 499-504, 1974
5	A Busemann	Das Förderhöhenverhältnis radialer Kreiselpumpen mit logarithmisch-spiraligen Schaufeln Z angew, Math Mech, Vol 8, pp 372-384, 1928
6	O E Baljé	A contribution to the problem of designing radial turbomachines Trans ASME, Vol 74, pp 451-472, 1952
7	F J Wiesner	A review of slip factors for centrifugal impellers J Engng Pwr Trans ASME A, Vol 89, pp 558-572, 1967
8	J Moore	A wake and an eddy in a rotating radial-flow passage Pt I: Experimental observations ASME Paper No 73-GT-57, 1973
9	J Moore	A wake and an eddy in a rotating radial-flow passage Pt II: Flow model ASME Paper No 73-GT-58, 1973
10	A Carrard	Sue le calcul des roues centrifuges Techq Mod, Vol XV, No 3, p 65, 1923
11	R C Dean, Jr Y Senoo	Rotating wakes in vaneless diffusers J Bas Engng Trans ASME, D, Vol 82, pp 563-574, 1960
12	D Eckardt	Instantaneous flow measurements in the jet-wake discharge flow of a centrifugal compressor impeller ASME Paper No 74-GT-90, 1974
13	I Man Moon	Effects of coriolis on turbulent flow in rotating rectangular channels MIT, Gas Turbine Laboratory Report No 89, 1967

REFERENCES (cont'd)

No	Author(s)	Title, etc
14	J P Johnston	The effects of rotation on boundary layers in turbo-machine rotors NASA SP-304, pp 207-249, 1974
15	P H Rothe J P Johnston	The effects of system rotation on separation, reattachment and performance in two-dimensional diffusers Stanford University, Dept Mech Eng, Thermosciences Div, Report PD-17, 1975
16	S A Eide J P Johnston	Prediction of the effects of longitudinal wall curvature and system rotation on turbulent boundary layers Stanford University, Dept Mech Eng, Thermosciences Div, Report PD-18, 1974
17	P G Schorr A D Welliver L J Winslow	Design and development of small high pressure ratio, single-stage centrifugal compressors "Advanced Centrifugal Compressors", ASME, 1971
18	H H Pearcey	Shock induced separation and its prevention by design and boundary "Boundary layer and flow control", Vol 2, Edited by G V Lachmann, Pergamon Press, New York, 1961
19	R E Morris D P Kenny	High pressure ratio centrifugal compressors for small gas turbine engines "Advanced Centrifugal Compressors", ASME, 1971
20	O E Baljé	A study on design criteria and matching of turbo-machines Pt B - Compressor and pump performance and matching of turbo components ASME Paper 60-WA-231, 1960
21	P H Timmis	Private communication
22	R W Fox S J Kline	Flow regimes in curved subsonic diffusers J Bas Engng Trans ASME, D, Vol 84, pp 303-316, 1962
23	L R Reneau J P Johnston S J Kline	Performance and design of straight two-dimensional diffusers Stanford University, Dept Mech Eng, Thermosciences Div, Report PD-8, 1964
24	A B Cocanower S J Kline J P Johnston	A unified method for predicting the performance of subsonic diffusers of several geometries Stanford University, Dept Mech Eng, Thermosciences Div, Report PD-10, 1965

REFERENCES (cont'd)

No	Author(s)	Title, etc
25	P W Runstadler, Jr R C Dean	Straight channel diffuser performance at high inlet Mach numbers J Bas Engng Trans ASME, D, Vol 91, pp 397-422, 1969
26	C J Sagi J P Johnston	The design and performance of two-dimensional curved diffusers ASME Paper No 67-FE-6, 1967
27	D P Kenny	A novel low cost diffuser for high performance centrifugal compressors ASME Paper No 68-GT-38, 1968
28	C. Rodgers H Mnew	Experiments with a model free-rotating vaneless diffuser ASME Paper No 74-GT-58, 1974
29	R C Pampreen	The use of cascade technology in centrifugal compressor vaned diffuser design ASME Paper No 72-GT-39, 1972
30	W Jansen	Rotating stall in a radial vaneless diffuser J Bas Engng Trans ASME, D, Vol 86, pp 750-758, 1964
31	C A Amann G E Nordenson G D Skellenger	Casing modification for increasing surge margin of a centrifugal compressor in an automotive turbine engine ASME Paper No 74-GT-92, 1974
32	D P Kenny	A comparison of the predicted and measured performance of high pressure ratio centrifugal compressor diffusers ASME Paper No 72-GT-54
33	R C Dean	The fluid dynamic design of advanced centrifugal compressors VKI Lecture Series, Advanced Radial Compressors, 1974
34	M G Jones D W Sparkes	Impeller Computer Design Package Pt I - A preliminary design program NGTE Internal Report, 1976
35	D J L Smith H Merryweather	Representation of the geometry of centrifugal impeller vanes by analytic surfaces NGTE Report No R322, 1973 and Intl Jnl for numerical methods in engineering, Vol 7, pp 137-154, 1973
36	C H Wu	A general theory of three-dimensional flow in subsonic and supersonic turbomachines of axial, radial and mixed-flow types NACA TN 2604, 1952

REFERENCES (cont'd)

No	Author(s)	Title, etc
37	J W Railly	Treatment of separated flow in cascades by a source distribution Proc Instn Mech Engrs, Vol 190, No 35, 1976
38	D P Sturge N Cumpsty	A two-dimensional method for calculating separated flow in centrifugal impellers J Fluids Engng Trans ASME, Vol 97, Series 1, No 4, December 1975
39	W J Calvert D J L Smith	A digital computer program for the subsonic flow past turbomachine blades using a matrix method NGTE Report No R328, November 1976
40	H Marsh	A digital computer program for the throughflow fluid mechanics in an arbitray turbomachine using a matrix method ARC R&M 3509, 1967
41	P M Came G T Kirby H Merryweather	Impeller Computer Design Package Part IV - The matrix throughflow program package NGTE Internal Report, 1975
42	W J Calvert P R Swinhoe	Impeller Computer Design Package Part VI - The application of finite element methods to the stressing of centrifugal impellers NGTE Internal Report, 1977
43	C J Parekh	Finite element computation system Part IV - Computer Report no 47 Dept of Civil Eng, University of Wales, September 1970

SK 117302

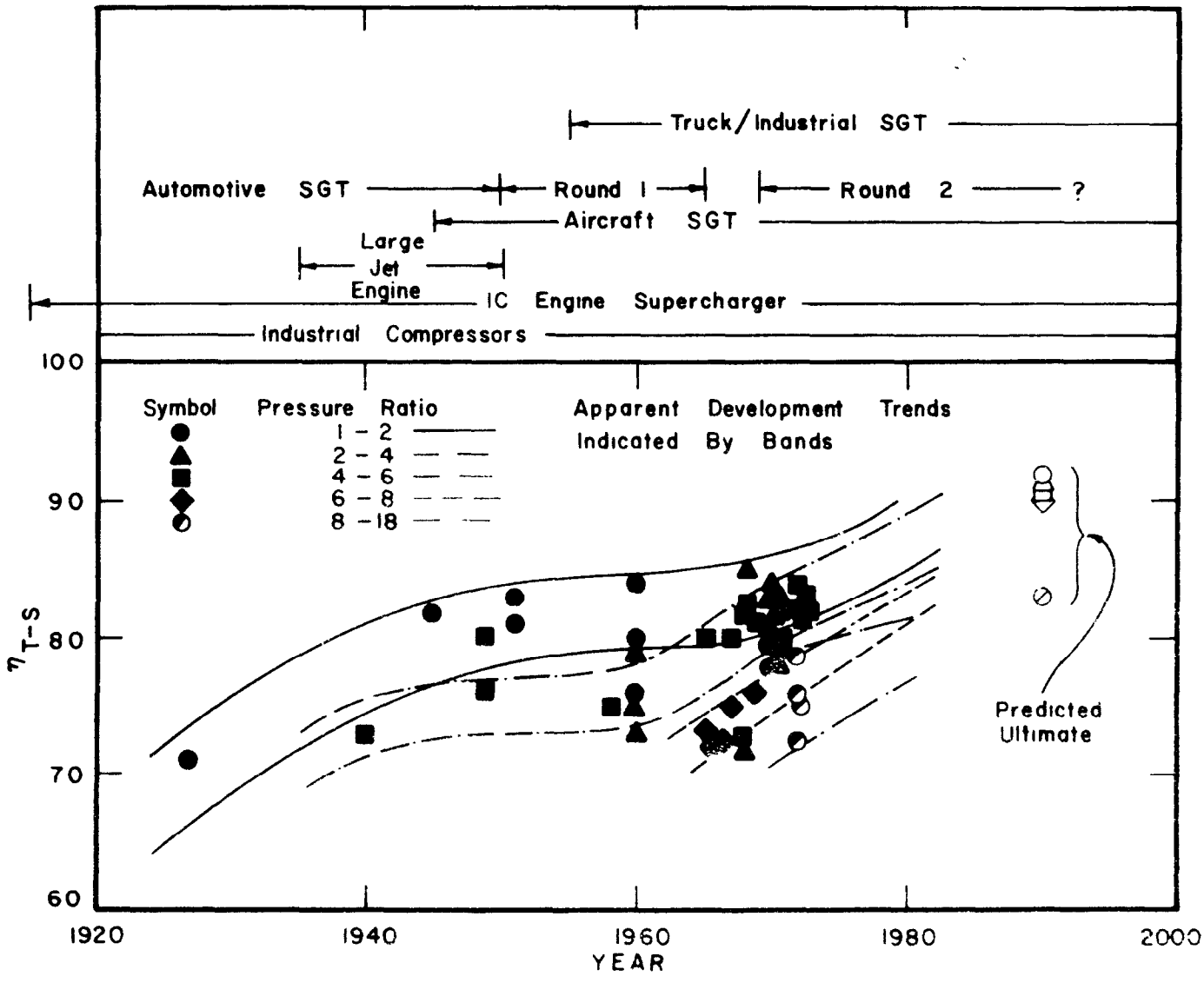

FIG.1 EVOLUTION OF THE CENTRIFUGAL COMPRESSOR (FROM DEAN, REF. 1)

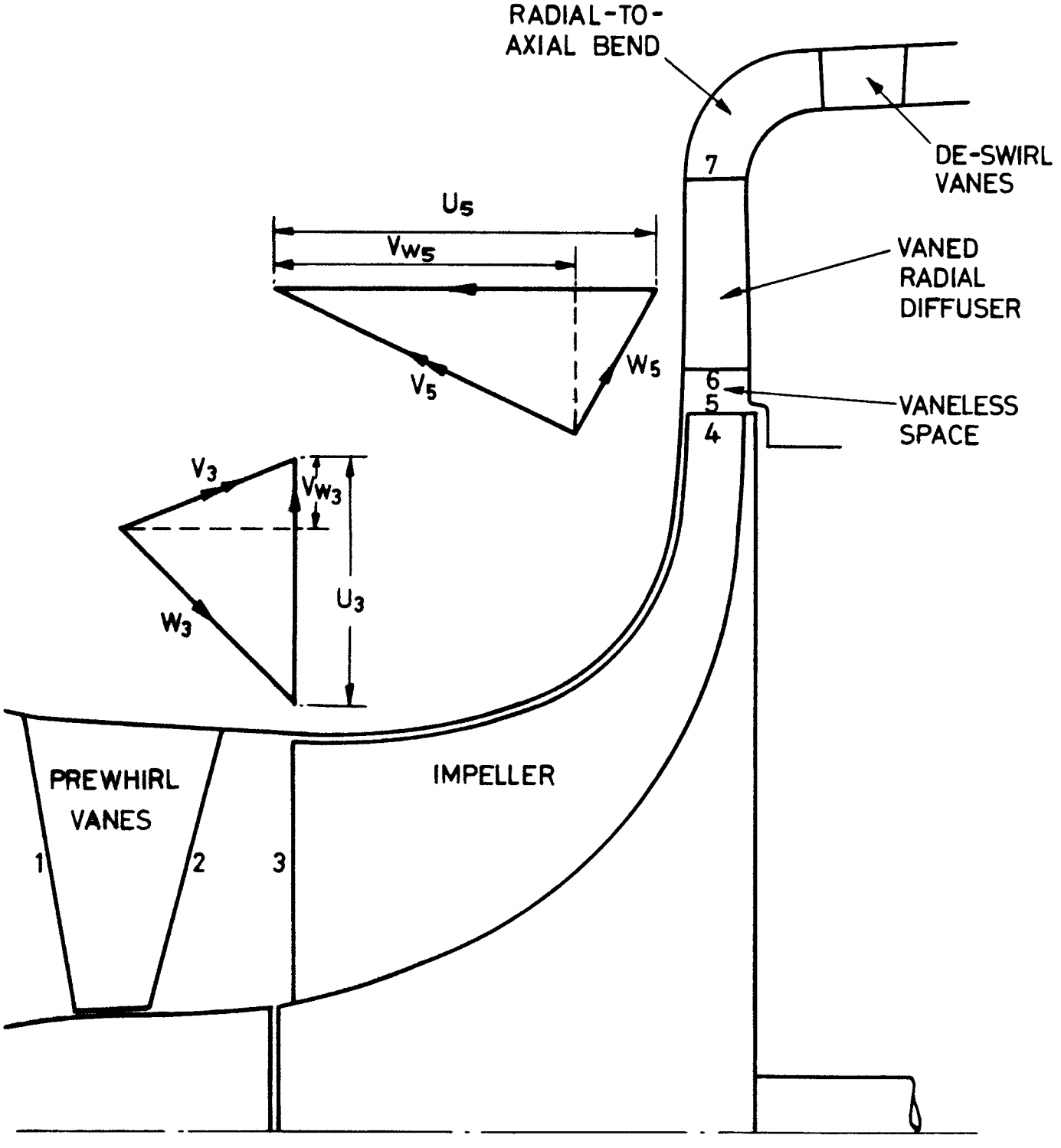

FIG. 2 NOMENCLATURE AND VELOCITY TRIANGLES

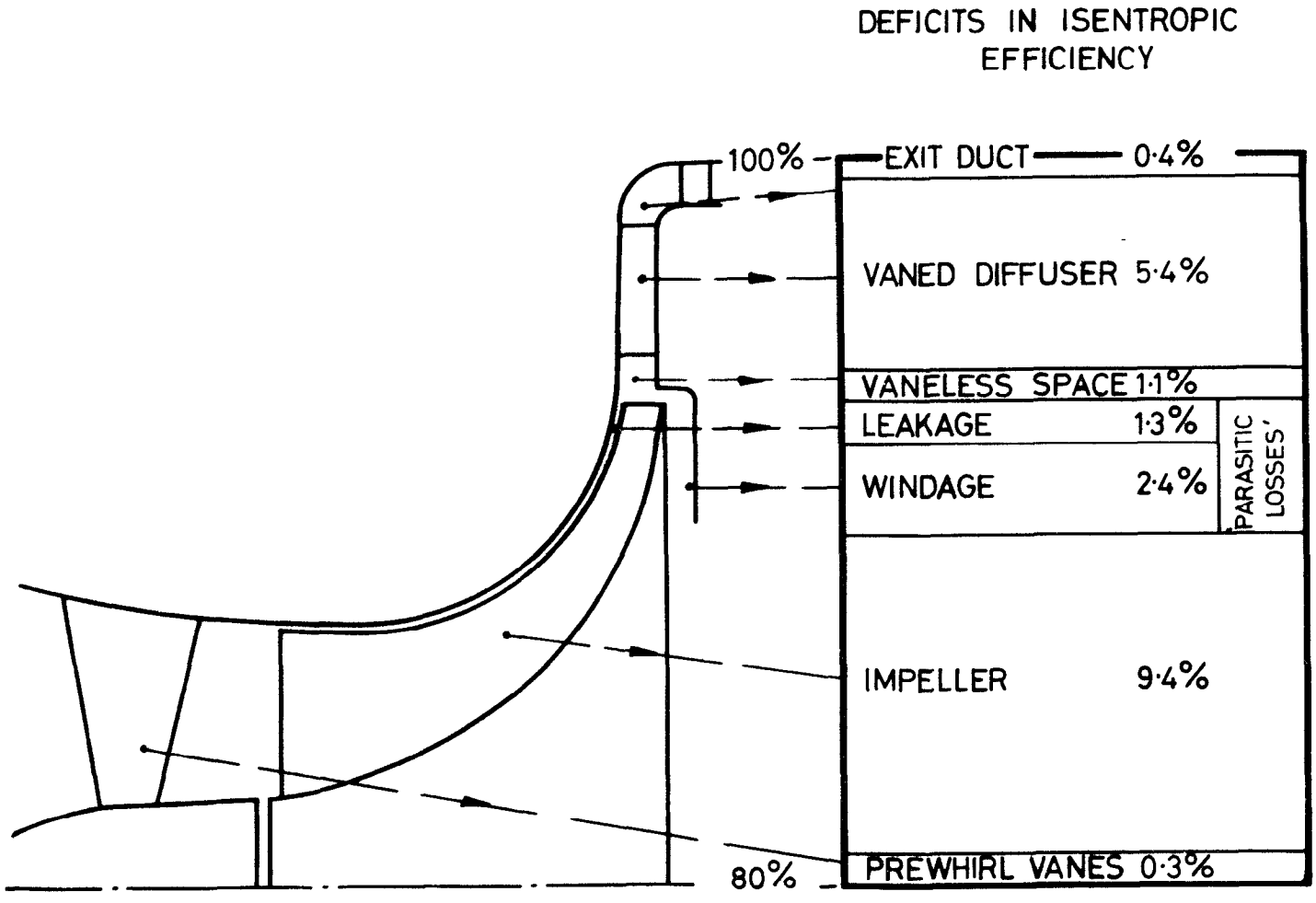

FIG. 3 LOSS BREAKDOWN
(8/1 PRESSURE RATIO COMPRESSOR)

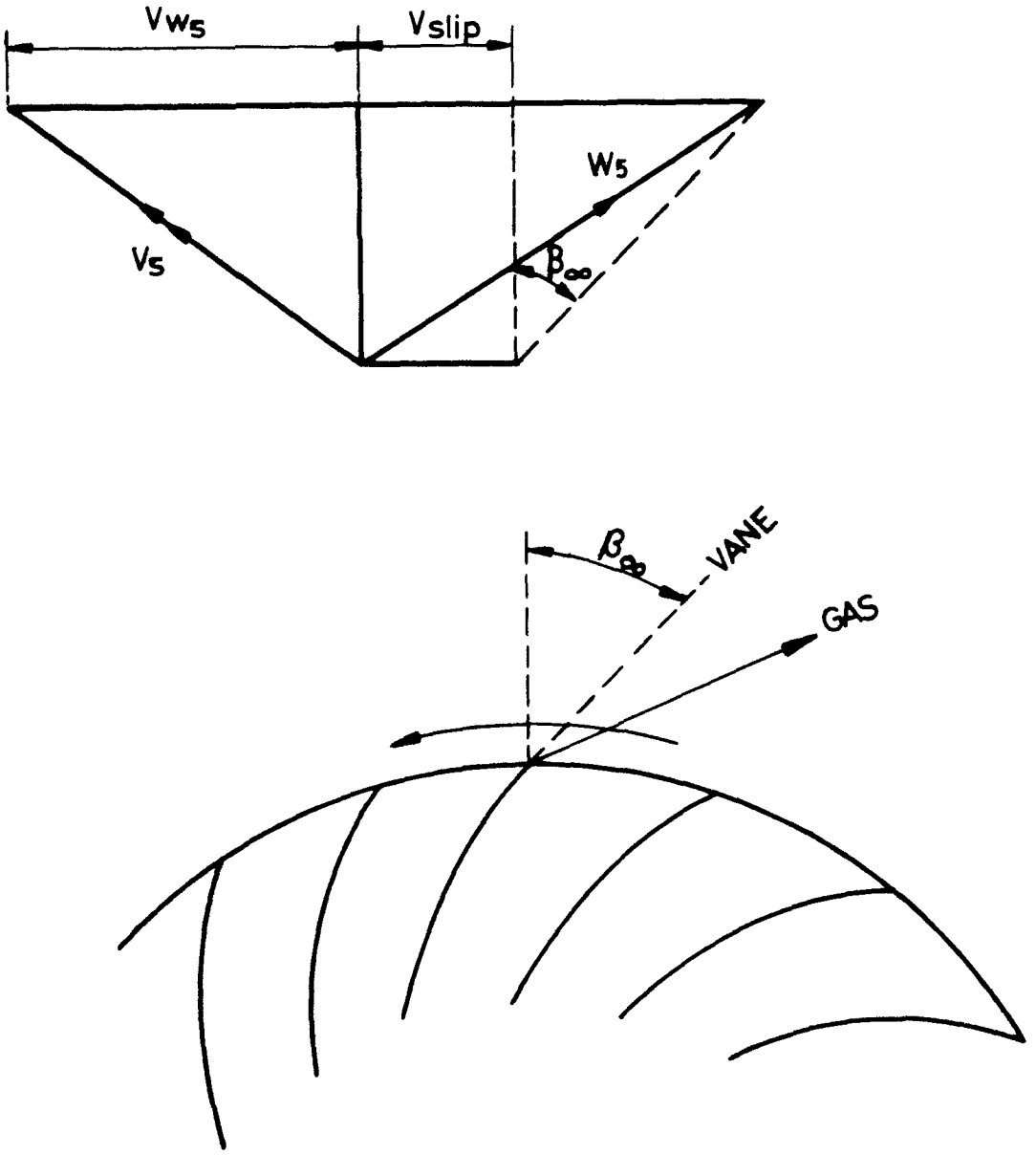

FIG. 4 EFFECT OF SLIP ON RELATIVE FLOW AT IMPELLER EXIT

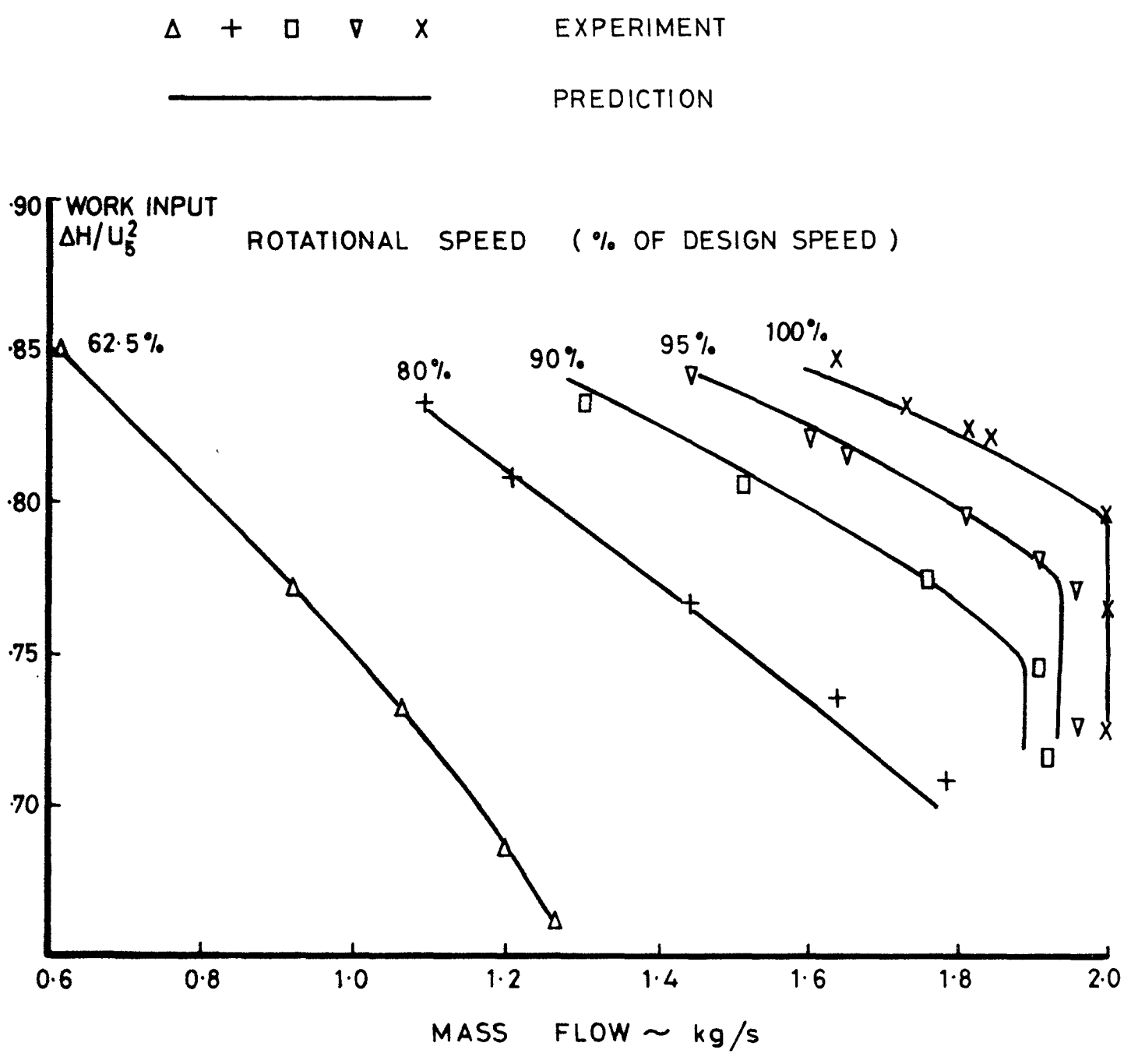

FIG. 5 PREDICTIONS OF WORK INPUT FOR THE IMPELLER OF A 6½/1 PRESSURE RATIO COMPRESSOR

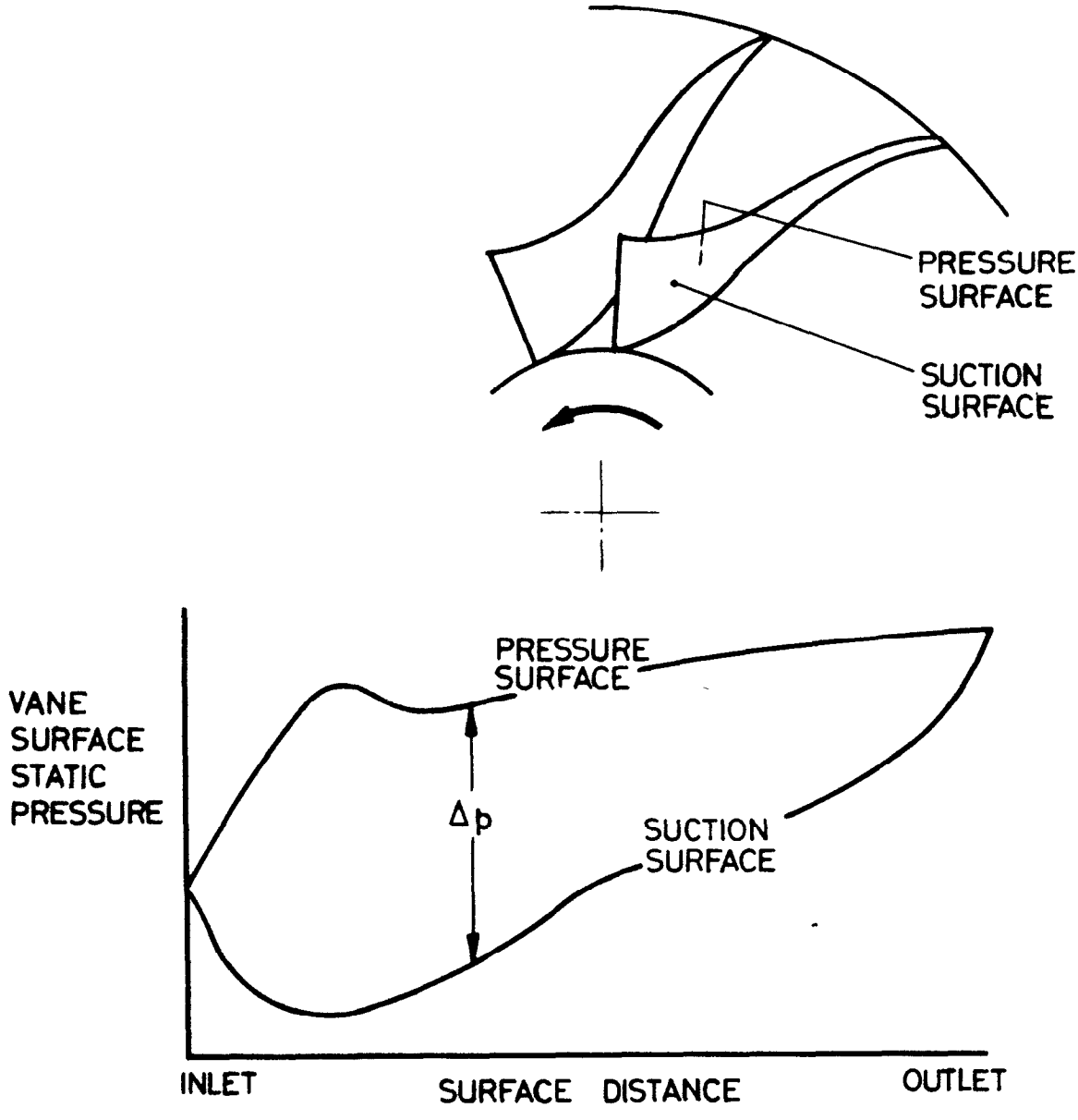

FIG. 6 VANE STATIC PRESSURE DISTRIBUTION

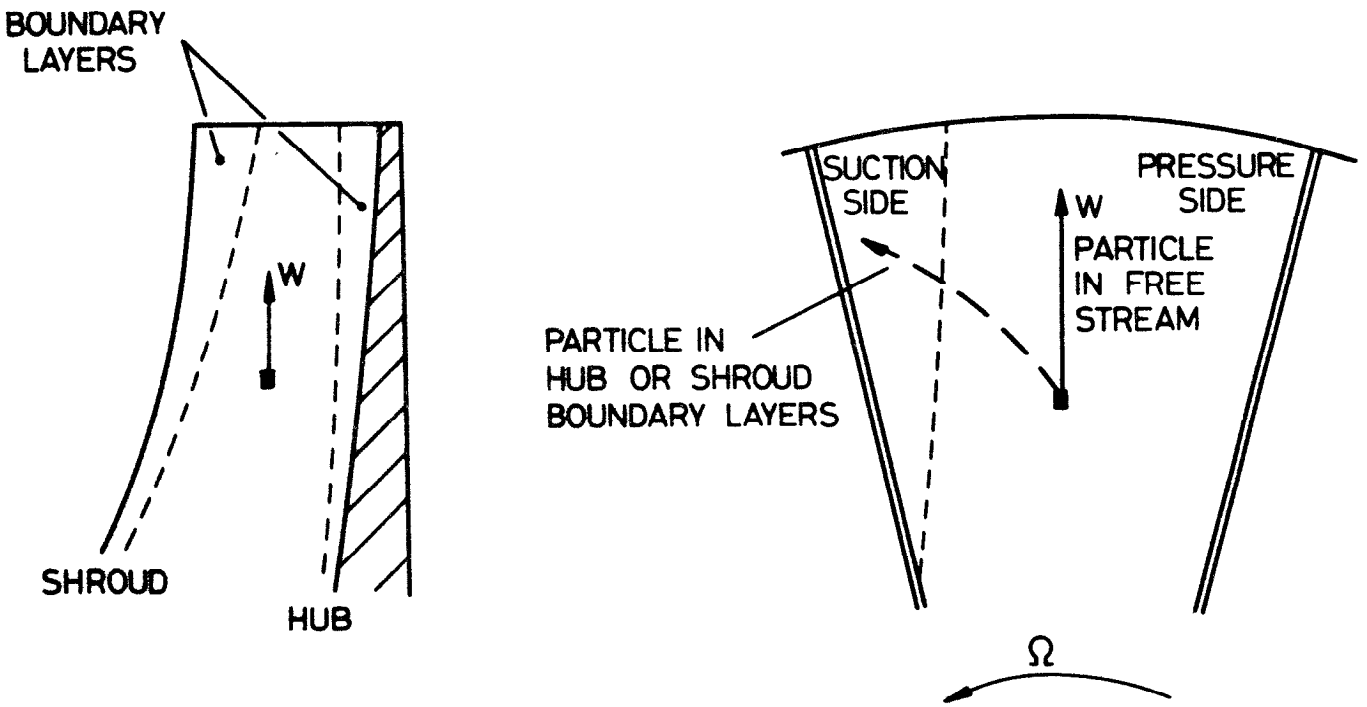

FIG.7 SECONDARY FLOW IN HUB AND SHROUD BOUNDARY LAYERS

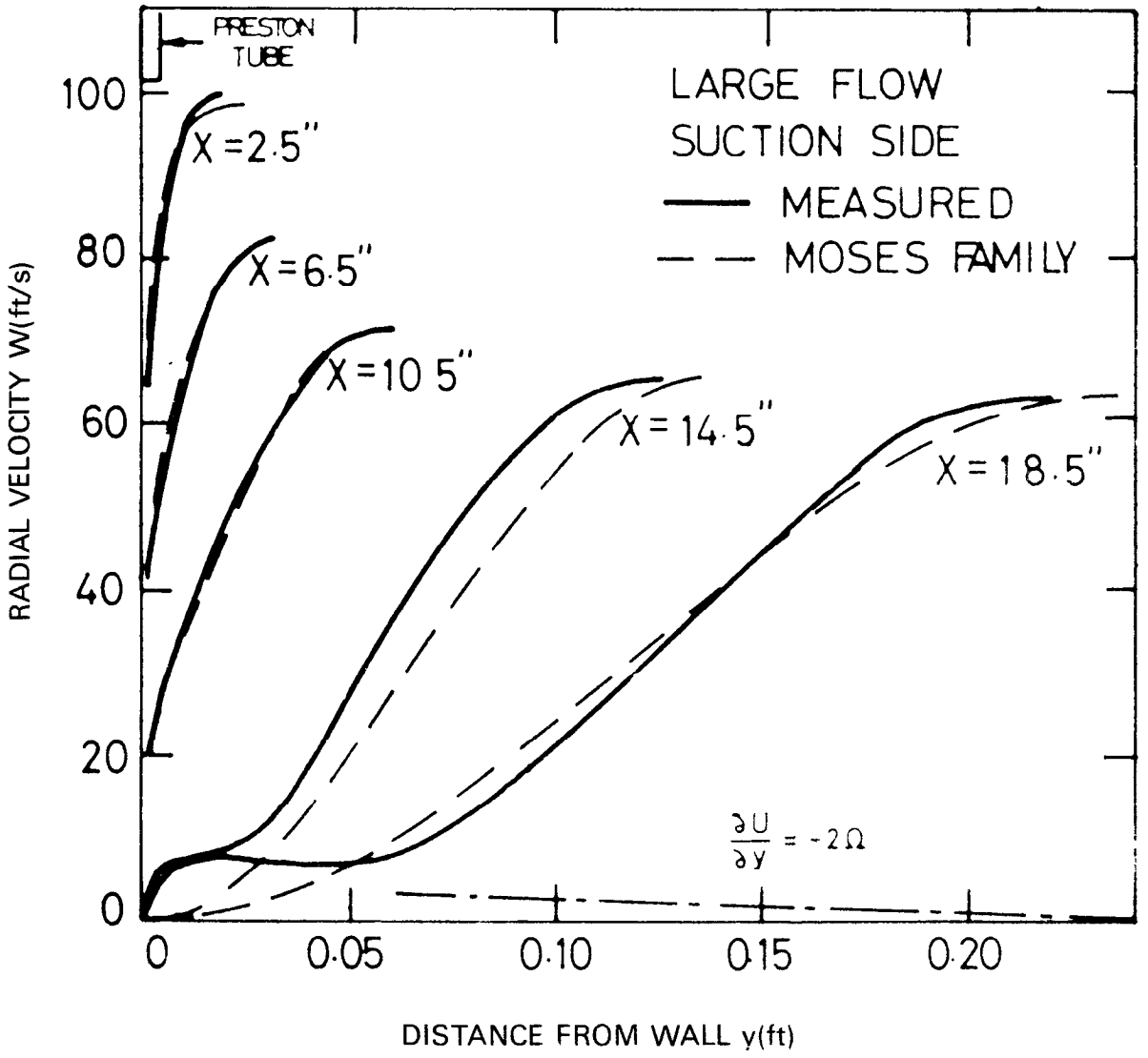

FIG. 8 BOUNDARY LAYER DEVELOPMENT ON SUCTION SURFACE OF MOORE'S ROTATING CHANNEL (REF 9)

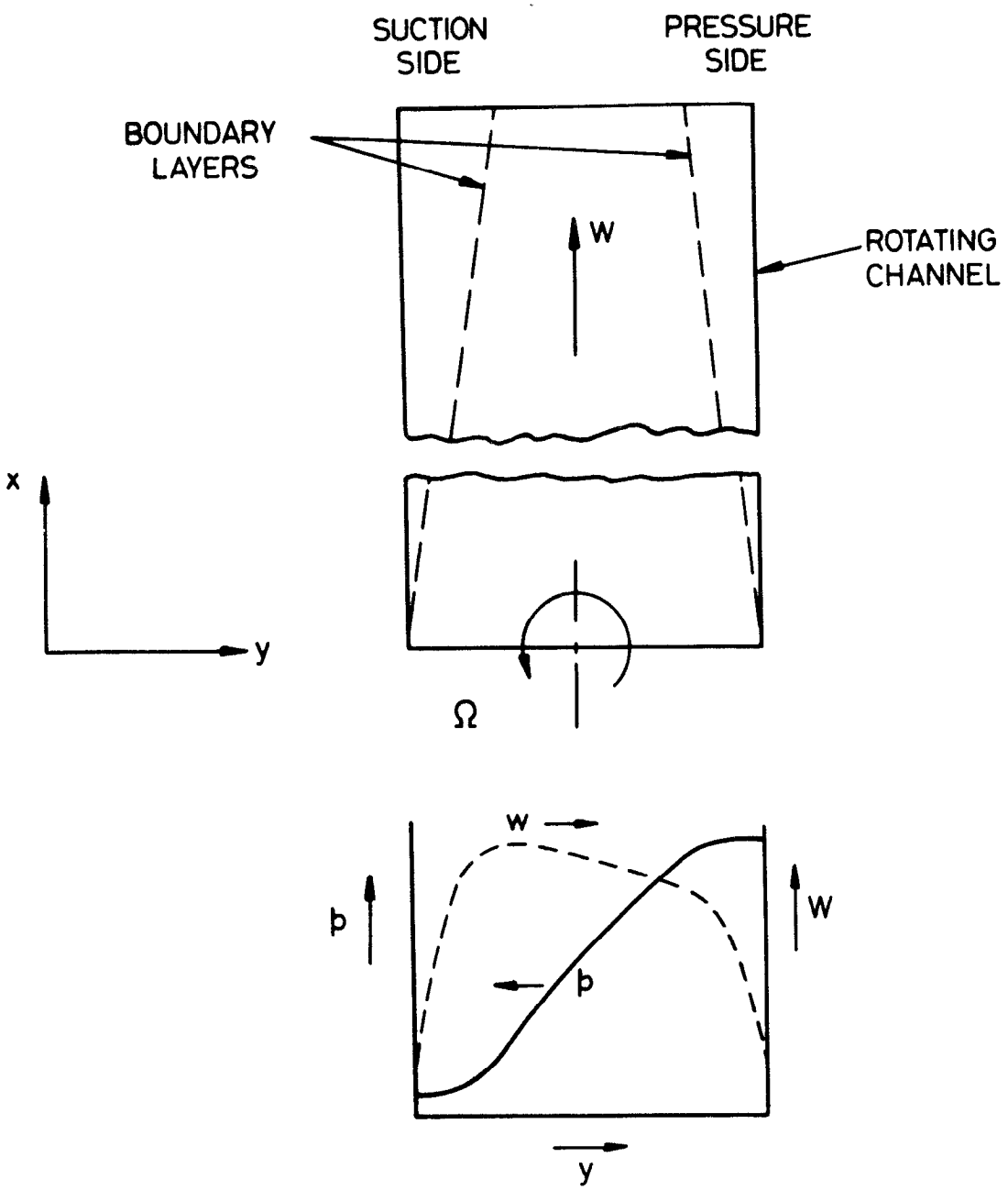

FIG. 9 ROTATING, RECTANGULAR, RADIAL-FLOW CHANNEL

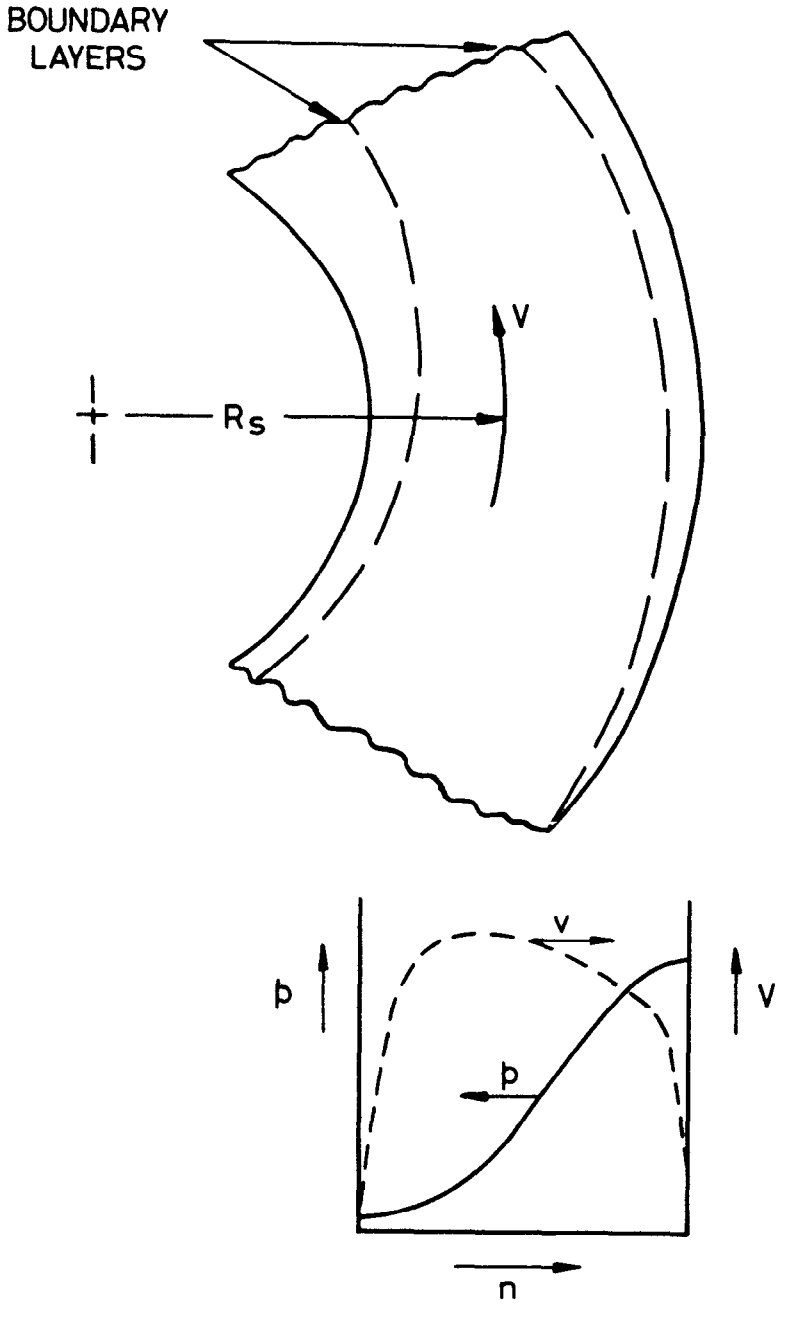

FIG. 10 CURVED, STATIONARY CHANNEL

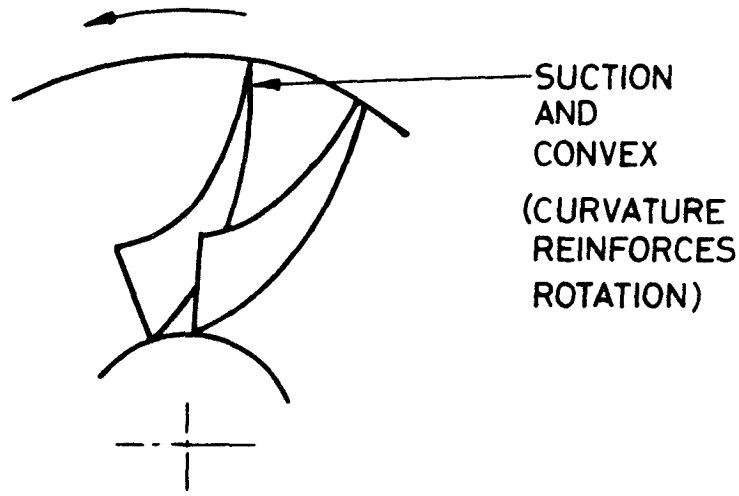

(a) RADIALLY BLADED IMPELLER

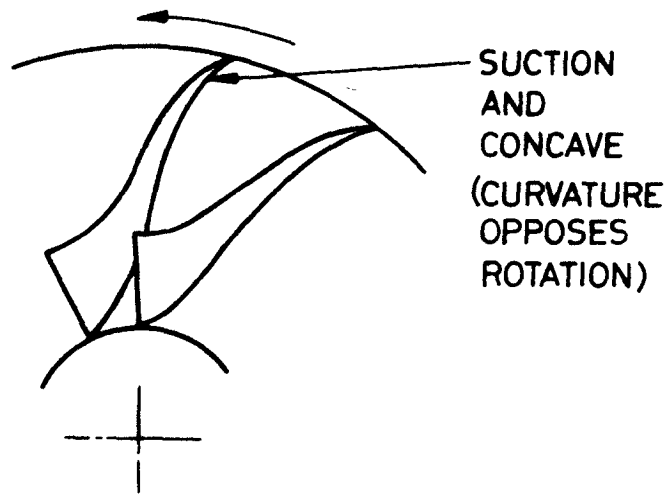

(b) SWEPT BACK IMPELLER

FIG. 11 EFFECT OF VANE SHAPE ON SUCTION SURFACE BOUNDARY LAYER

117632

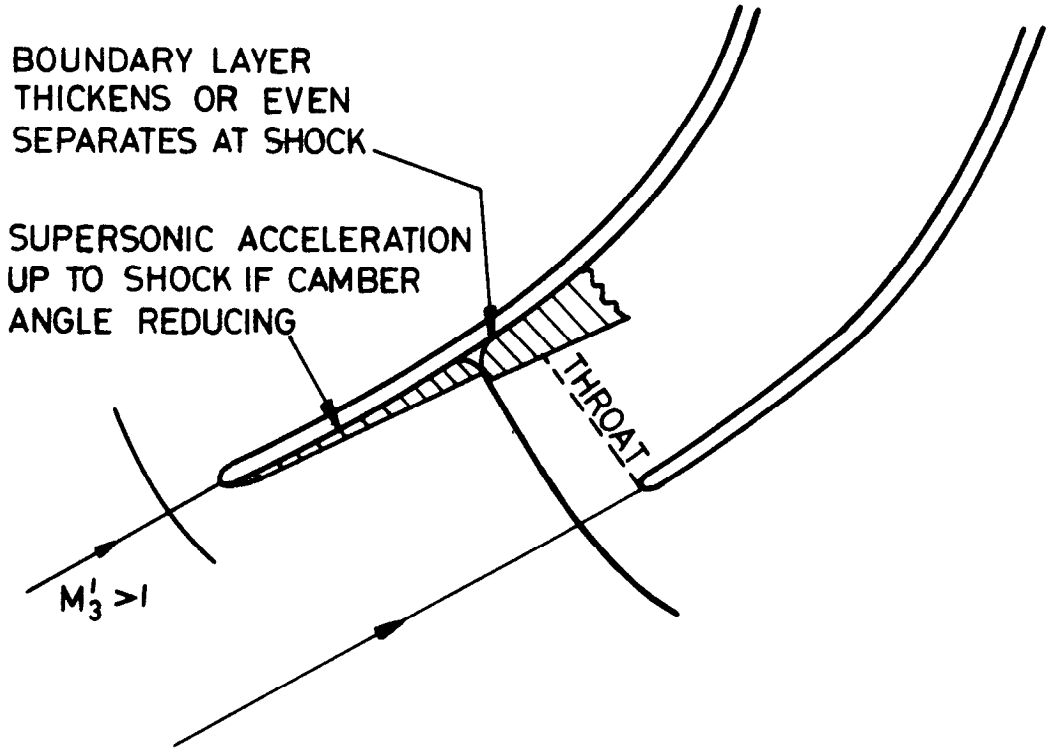

(a) ZERO INCIDENCE

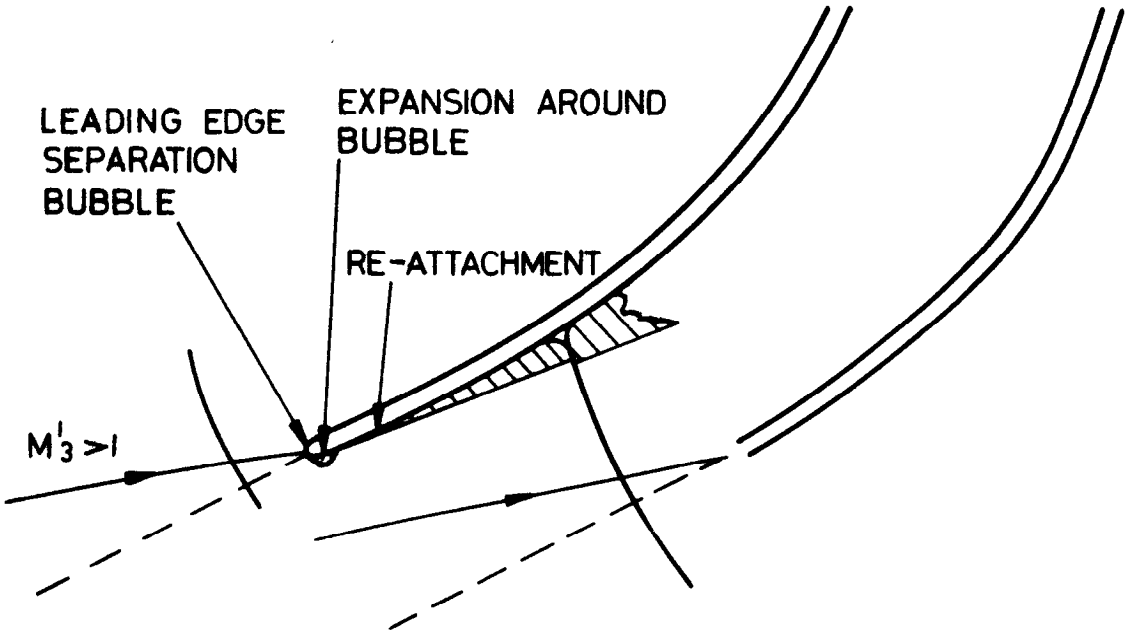

(b) POSITIVE INCIDENCE

FIG. 12 INDUCER FLOW WITH TRANSONIC APPROACH MACH NUMBERS

SK 117633

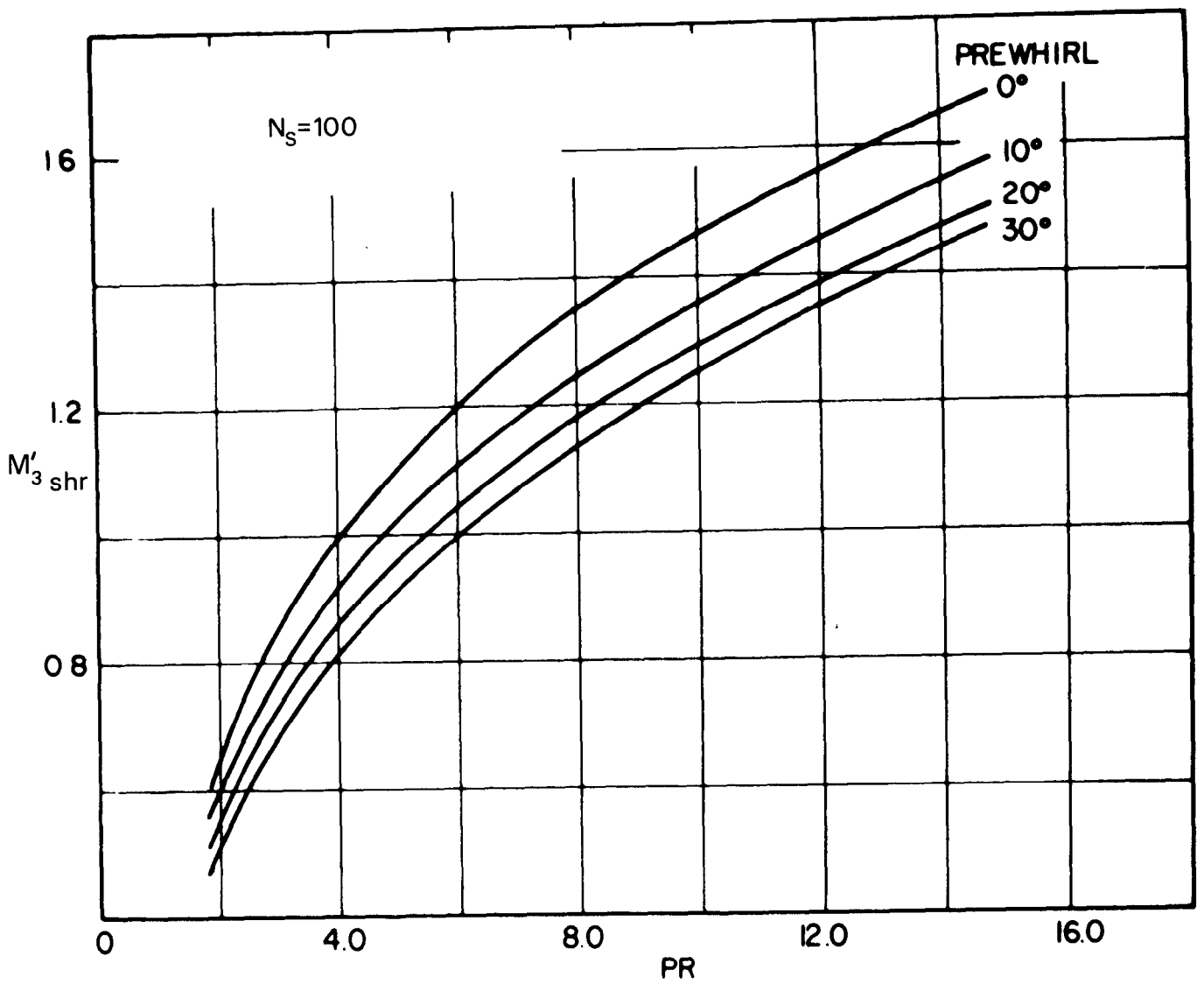

FIG.13 VARIATION OF SHROUD INLET RELATIVE MACH NUMBER WITH PRESSURE RATIO AND PREWHIRL ANGLE (REF 19)

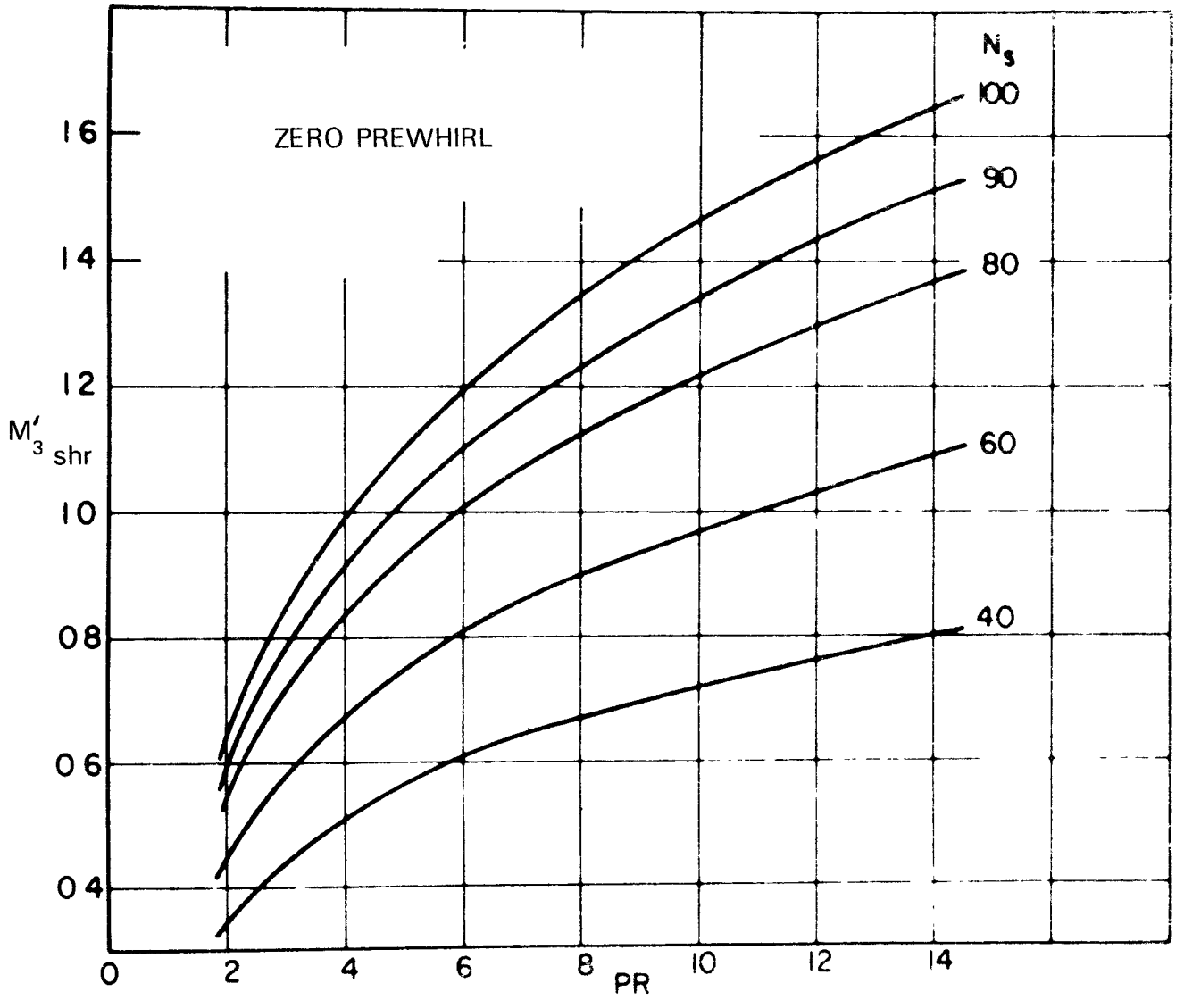

FIG.14 VARIATION OF SHROUD INLET RELATIVE MACH NUMBER WITH PRESSURE RATIO AND SPECIFIC SPEED. (REF 19)

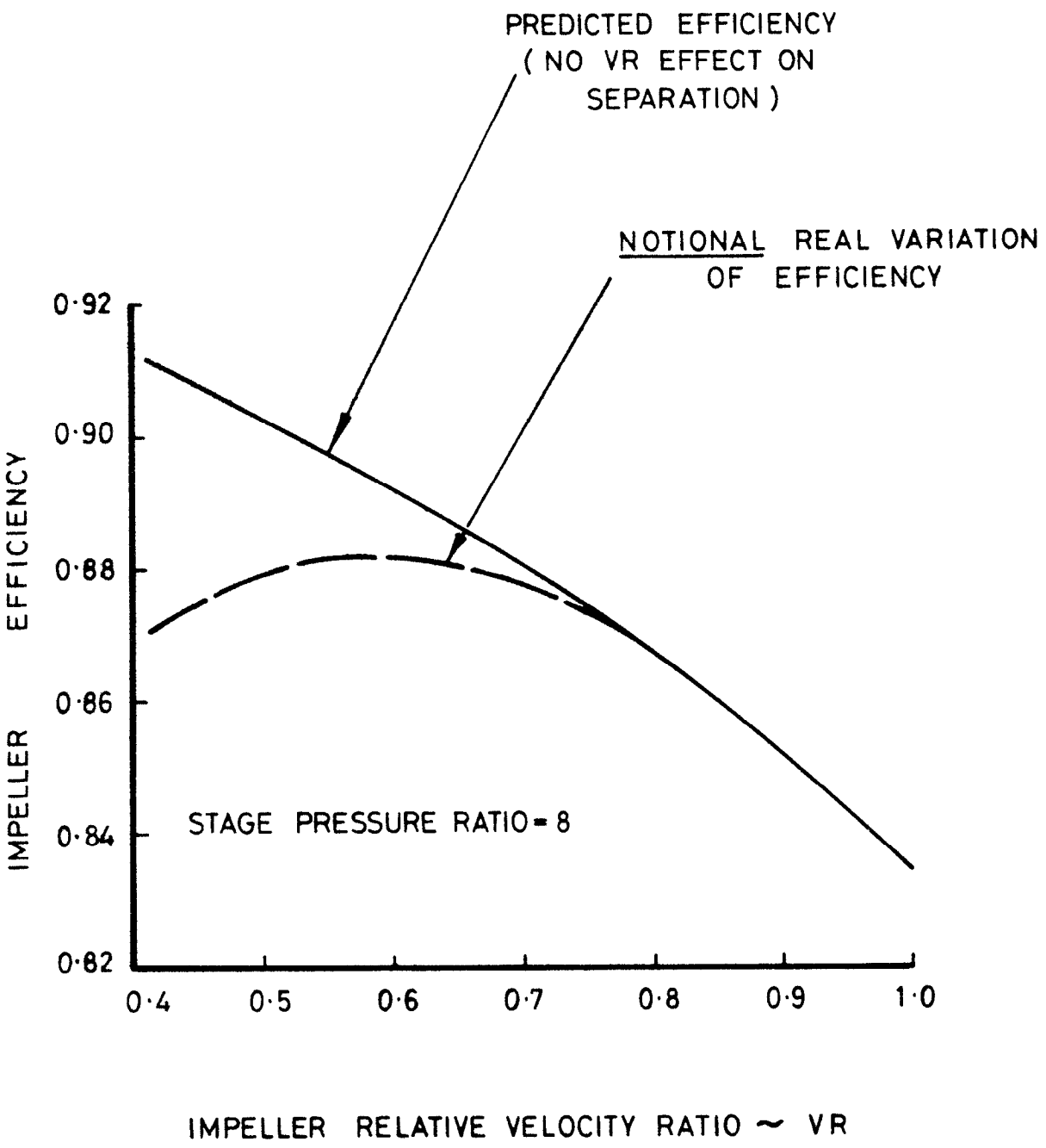

FIG. 15 EFFECT OF VELOCITY RATIO ON IMPELLER EFFICIENCY

SK 117636

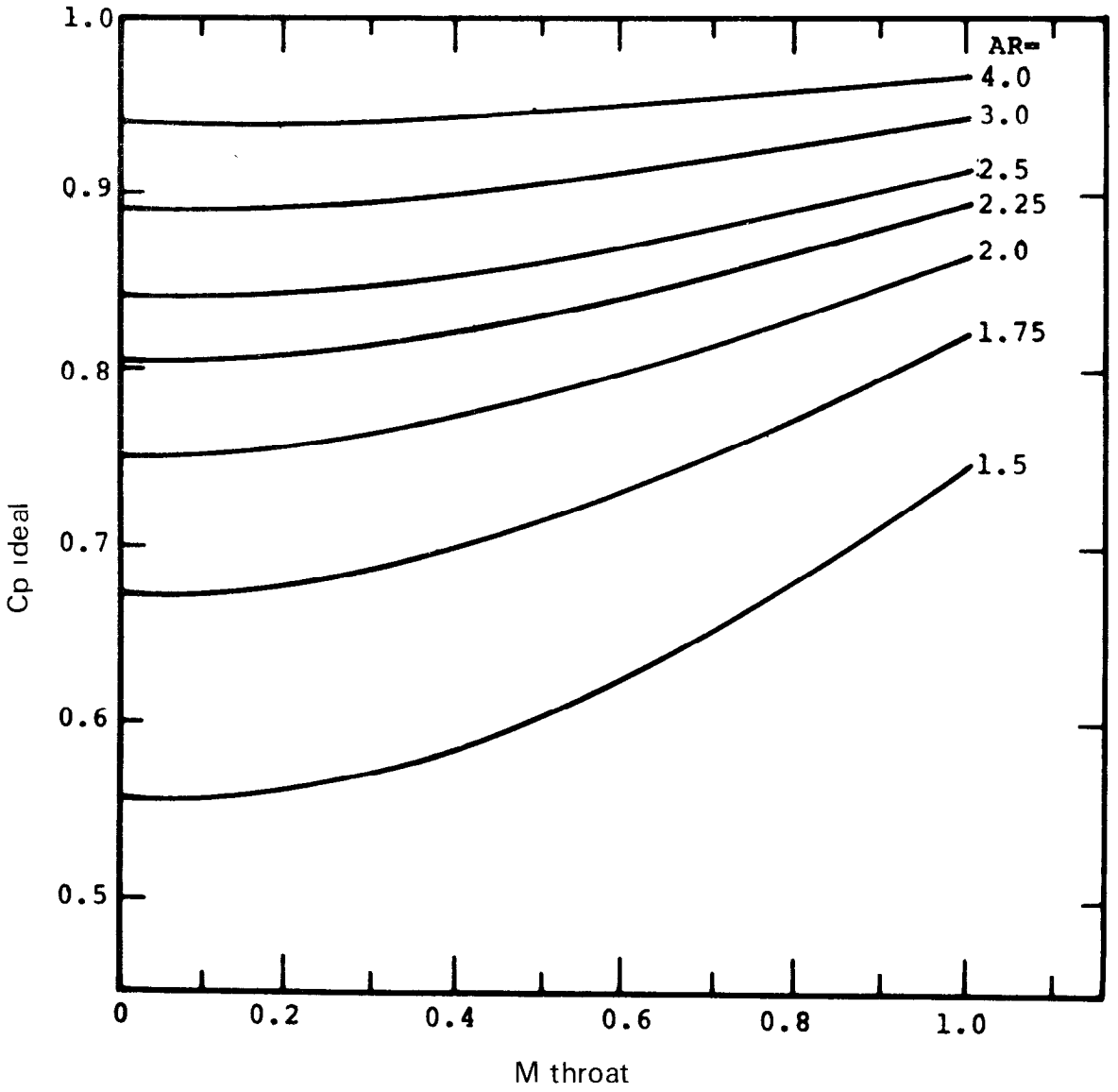

FIG.16 VARIATION OF IDEAL PRESSURE RECOVERY WITH THROAT MACH NUMBER AND AREA RATIO (REF 25)

SK 117637

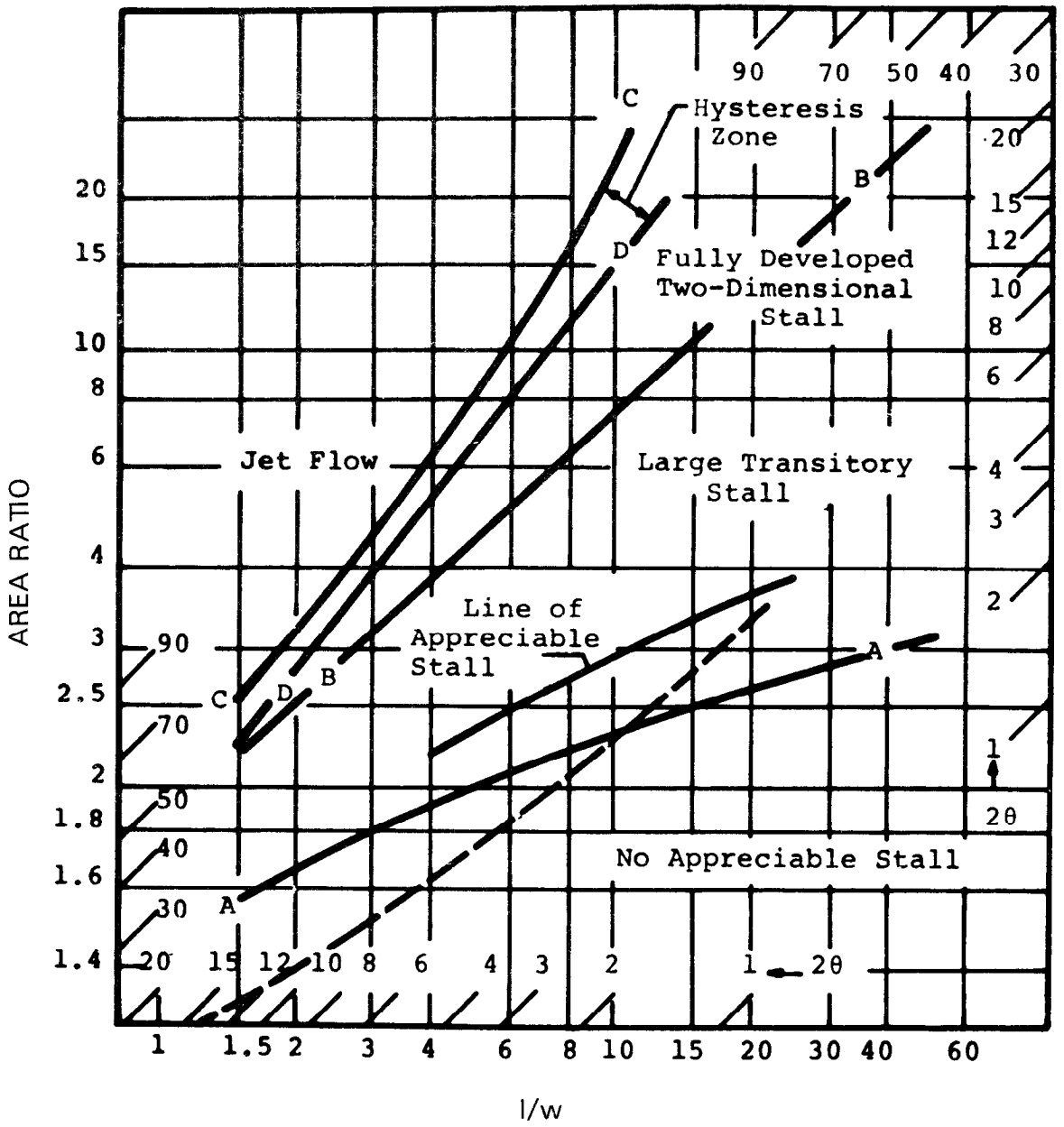

FIG.17 FLOW REGIMES ESTABLISHED BY FOX AND KLINE (REF 22)

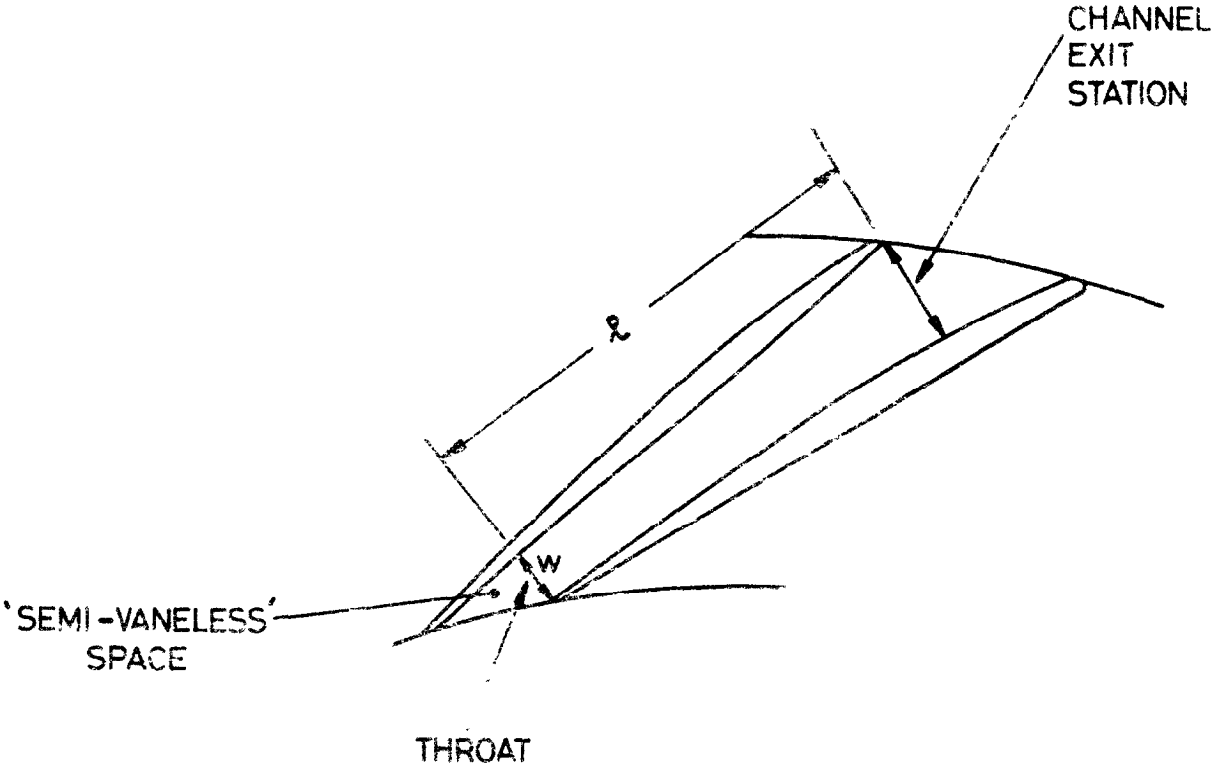

AREA RATIO (AR) = EXIT AREA / THROAT AREA

FIG. 18 DIFFUSER NOMENCLATURE

SK 117639

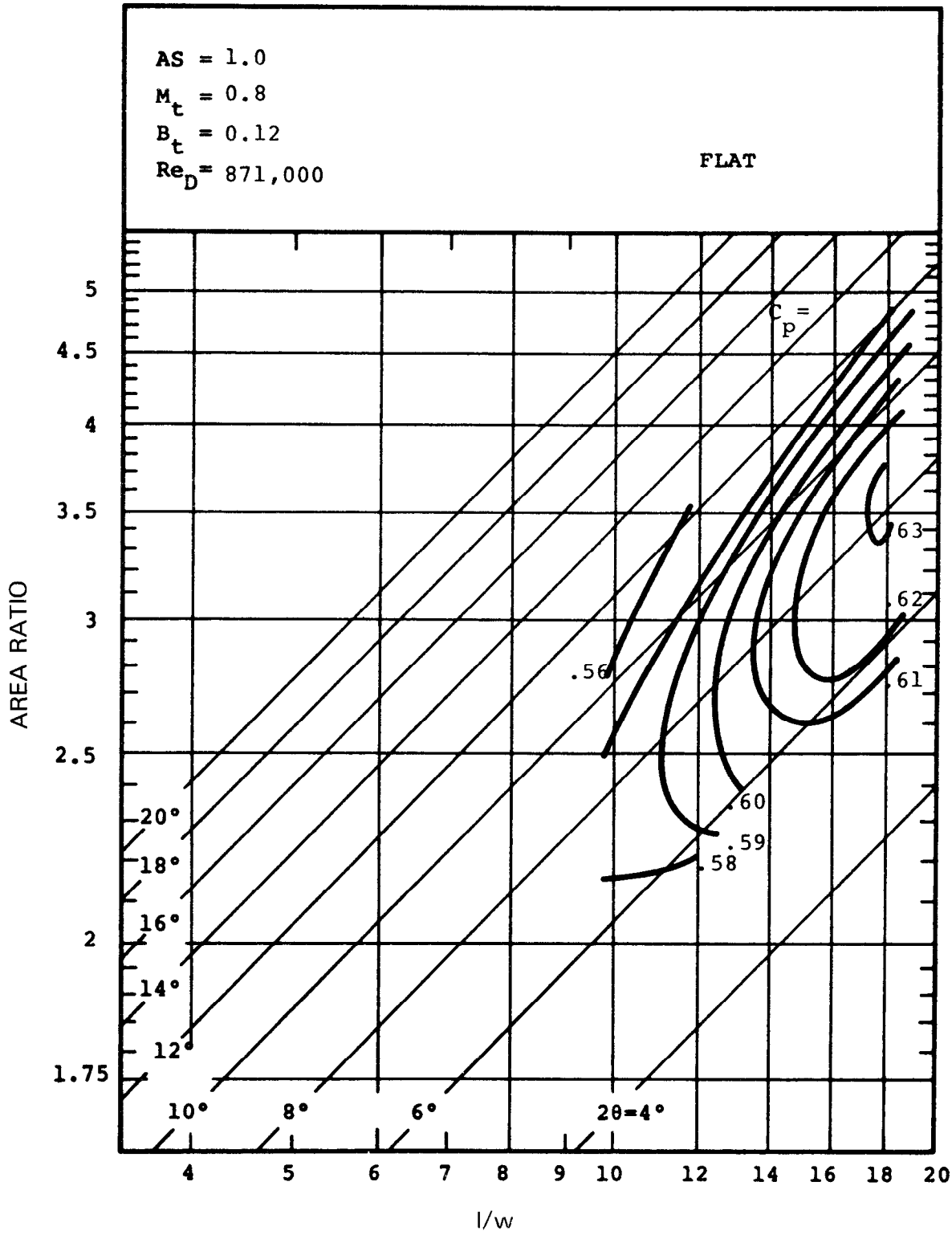

FIG.19 EXAMPLE OF EXPERIMENTAL Cp CONTOURS OBTAINED BY RUNSTADLER (REF 25)

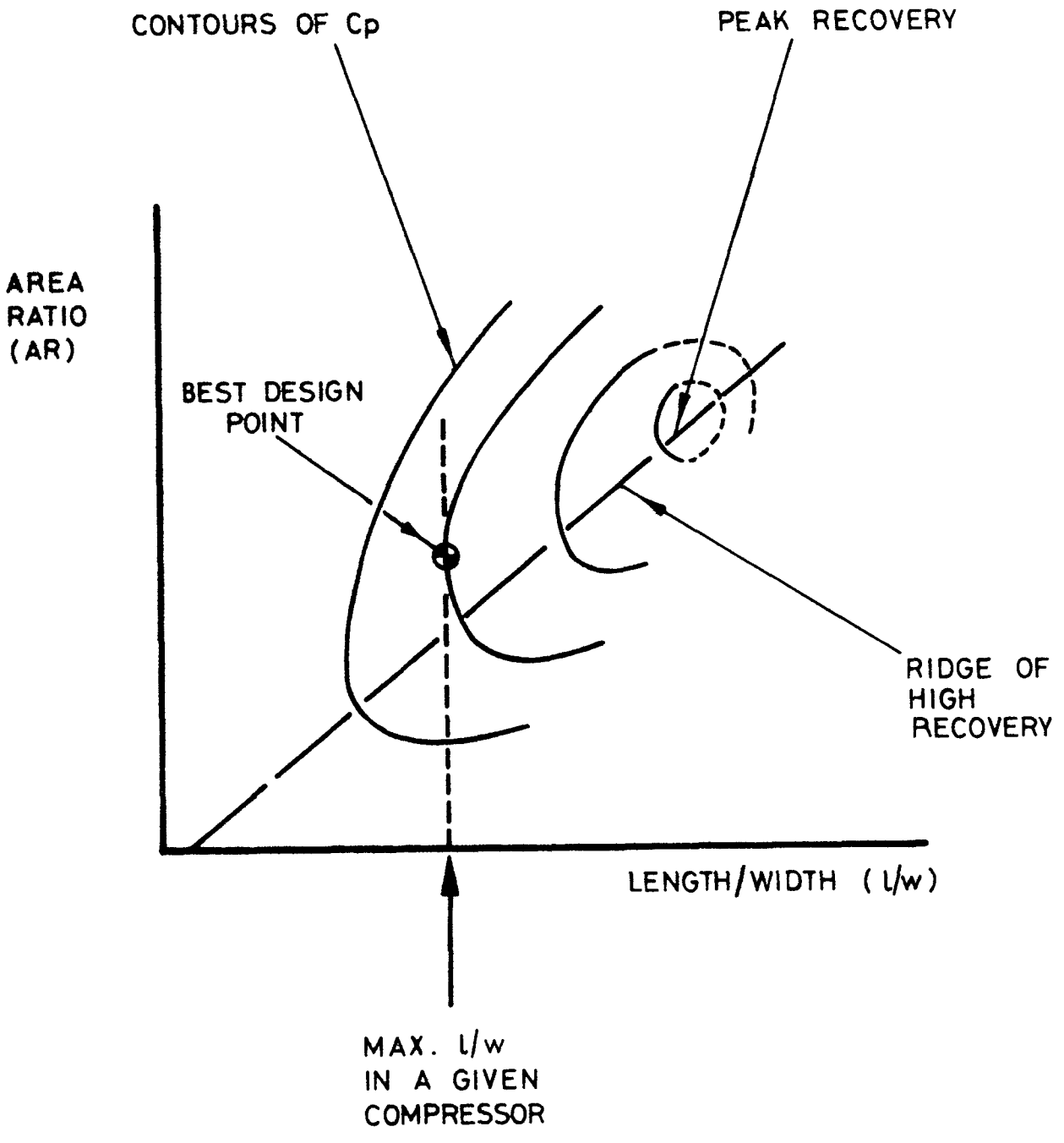

FIG. 20 CHOICE OF GEOMETRY OF VANED DIFFUSER OF FIXED RADIAL CONSTRAINT

117641

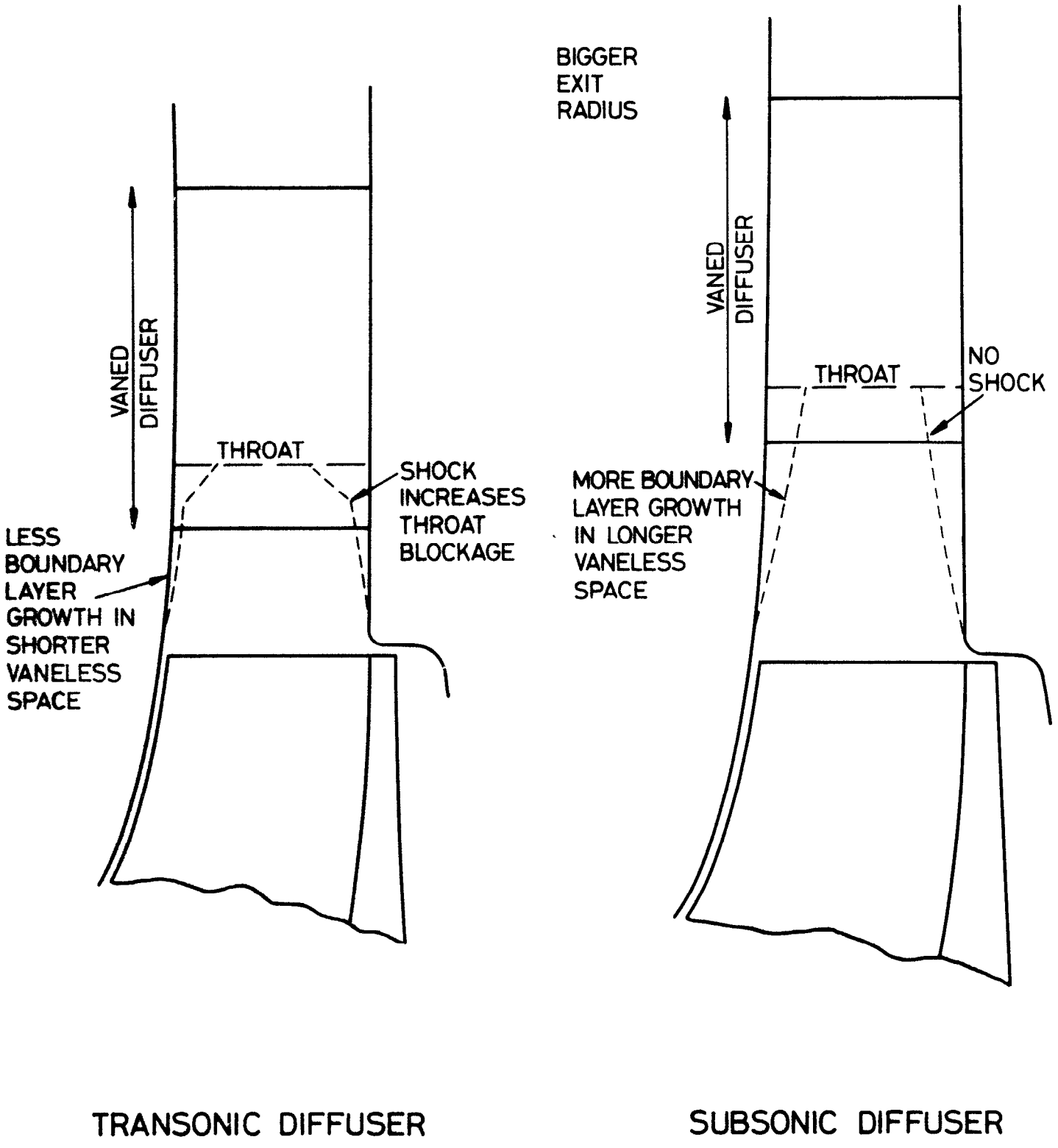

FIG. 21 CHOICE OF DIFFUSER APPROACH CONDITIONS

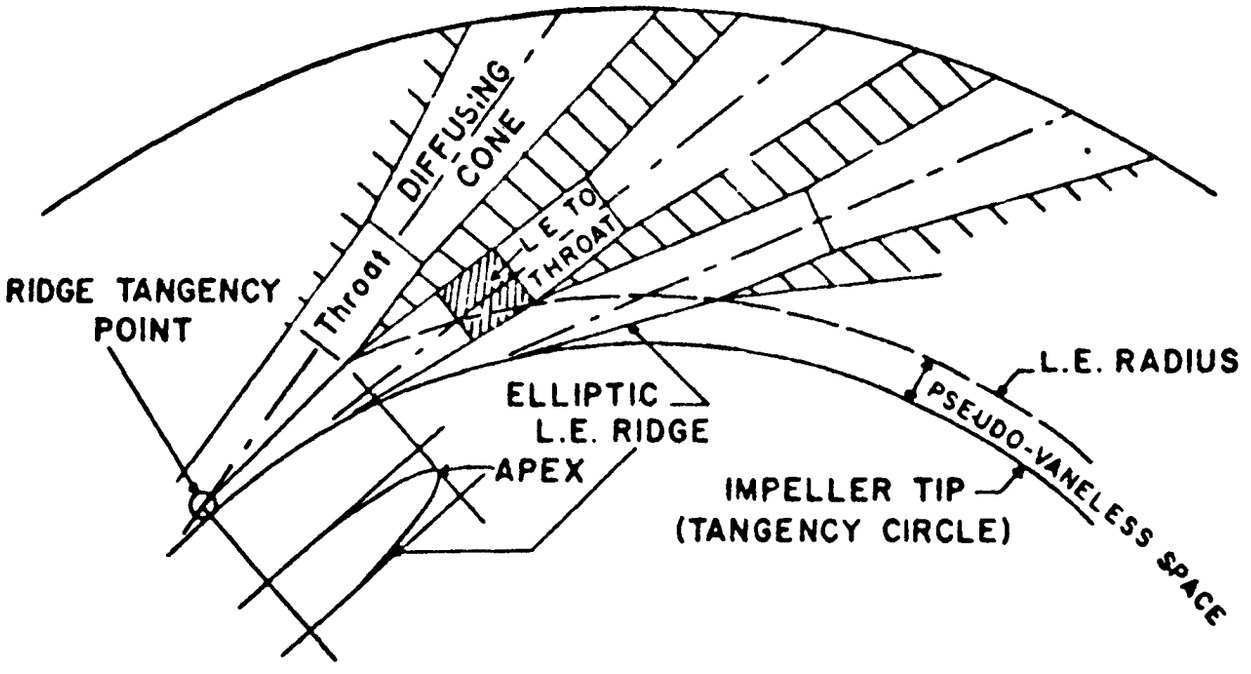

FIG.22 THE PIPE DIFFUSER (REF 27)

SK 117643

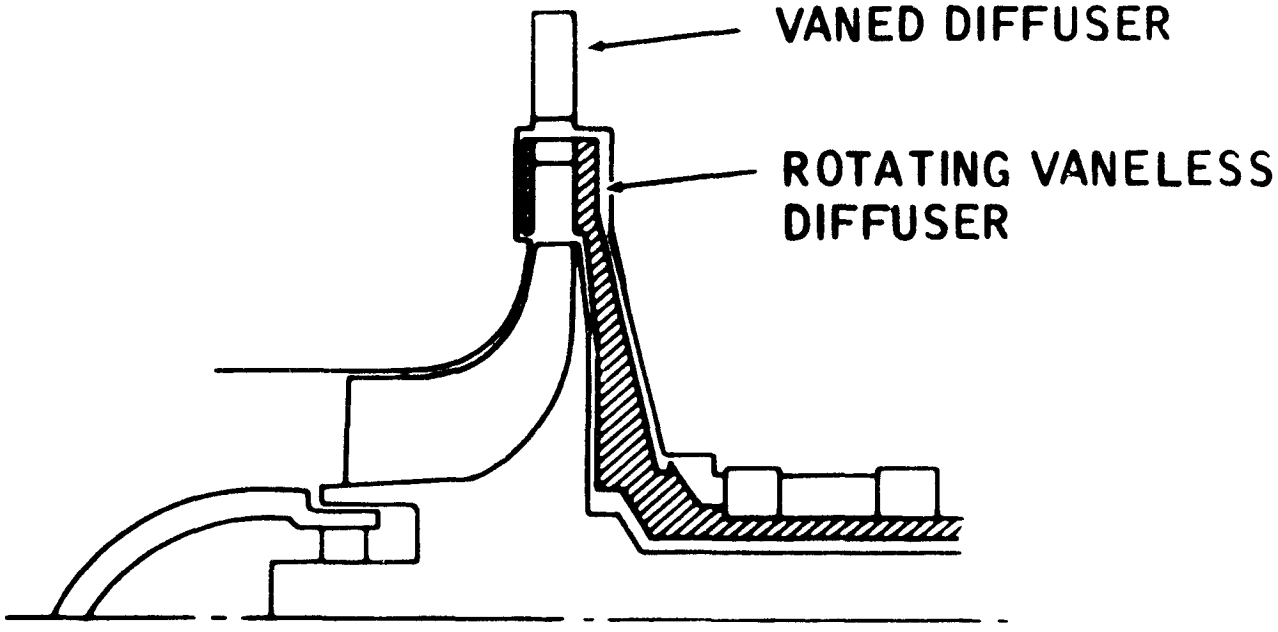

ROTATING WALL DIFFUSER

FIG.23 THE FREE-ROTATING VANELESS DIFFUSER. (REF 28)

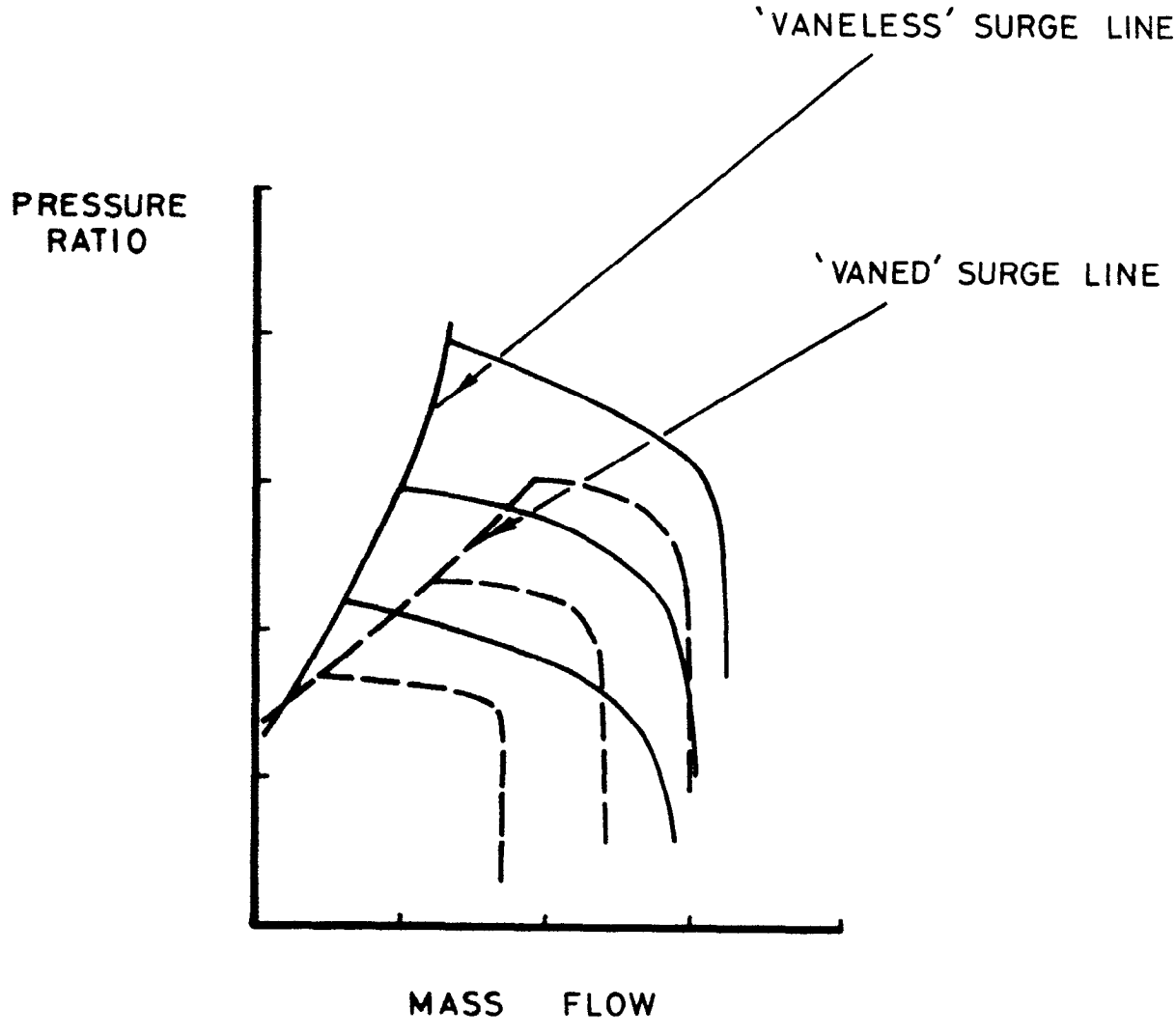

FIG. 24 SURGE OF VANED AND VANELESS DIFFUSER BUILDS OF A 6/1 PRESSURE RATIO COMPRESSOR

SK 117645

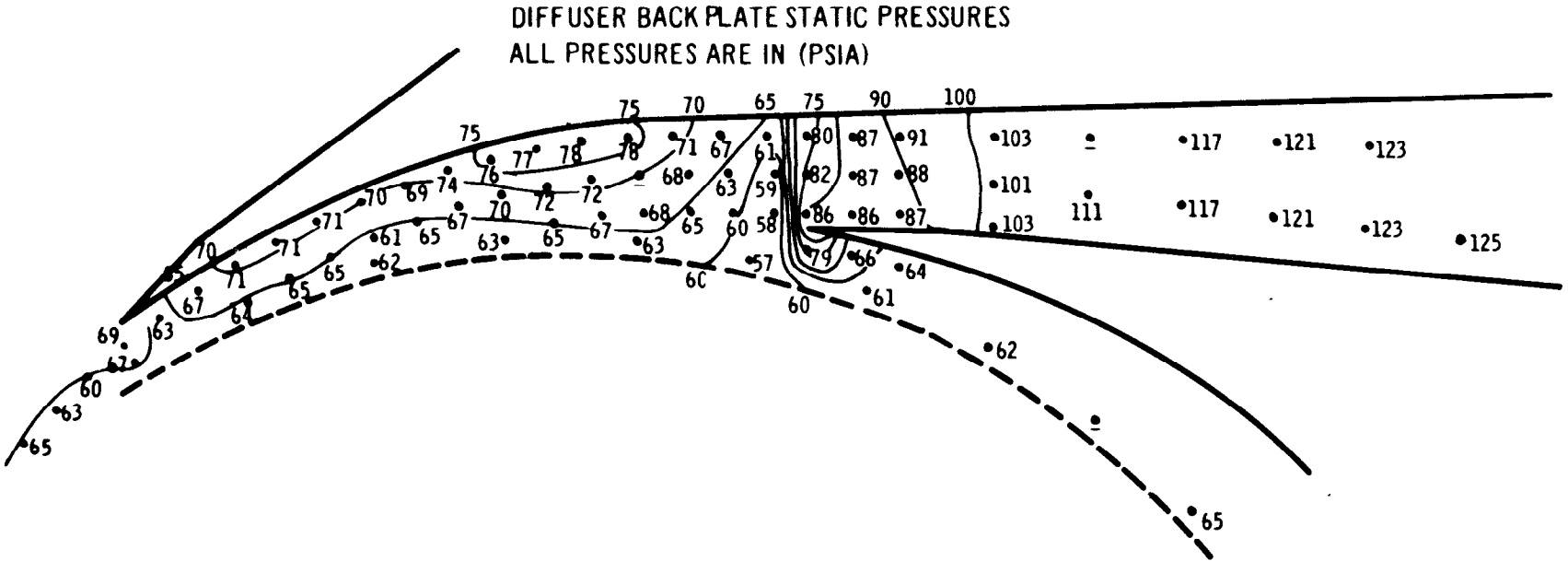

FIG.25 VANELESS SPACE PRESSURE FIELD (REF 17)

SK 117646

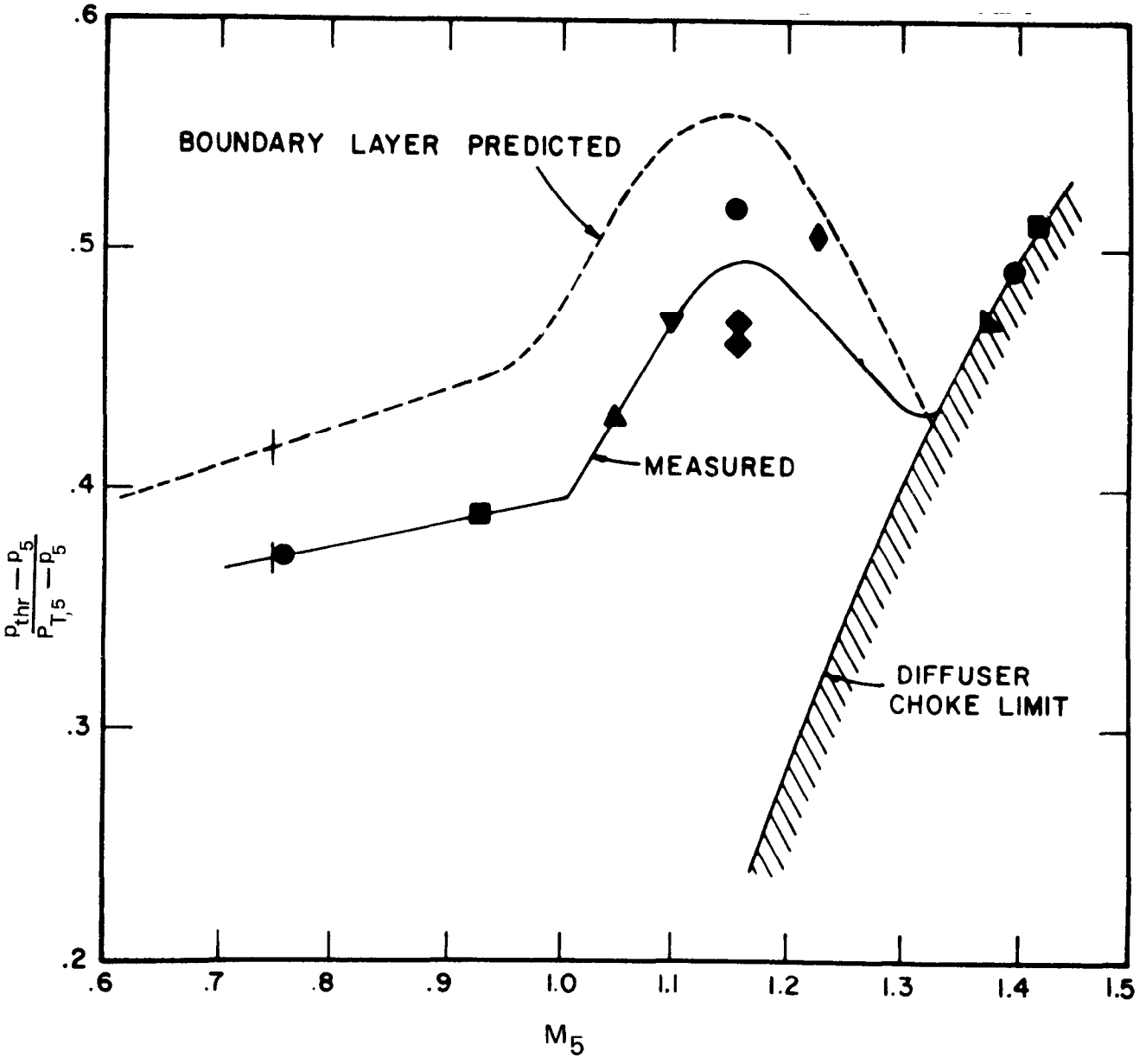

FIG.26 KENNY SURGE CORRELATION

117647

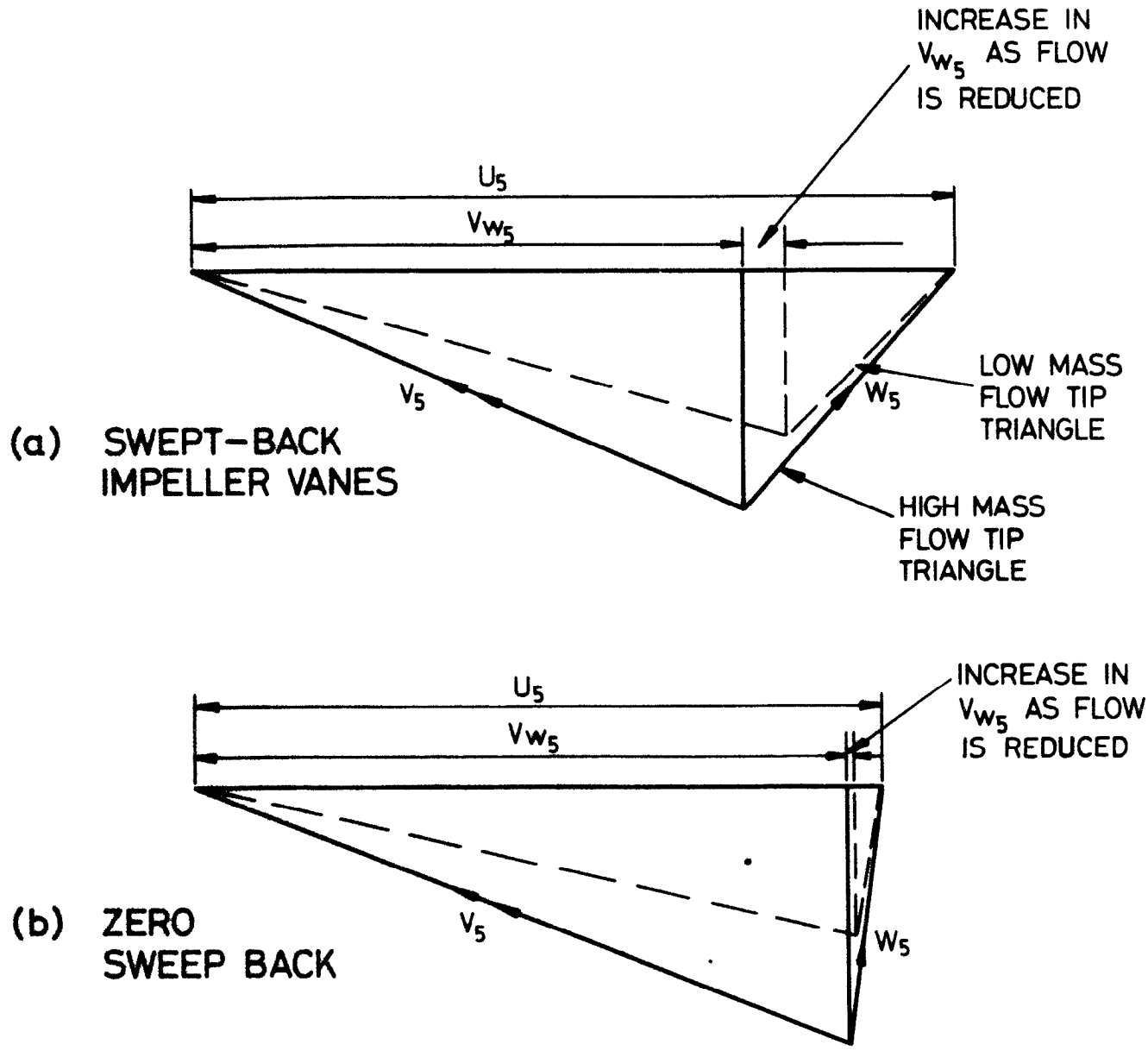

FIG. 27 EFFECT OF MASS FLOW DECREASE ON IMPELLER TIP VELOCITY TRIANGLE AND WORK INPUT

SK 117648

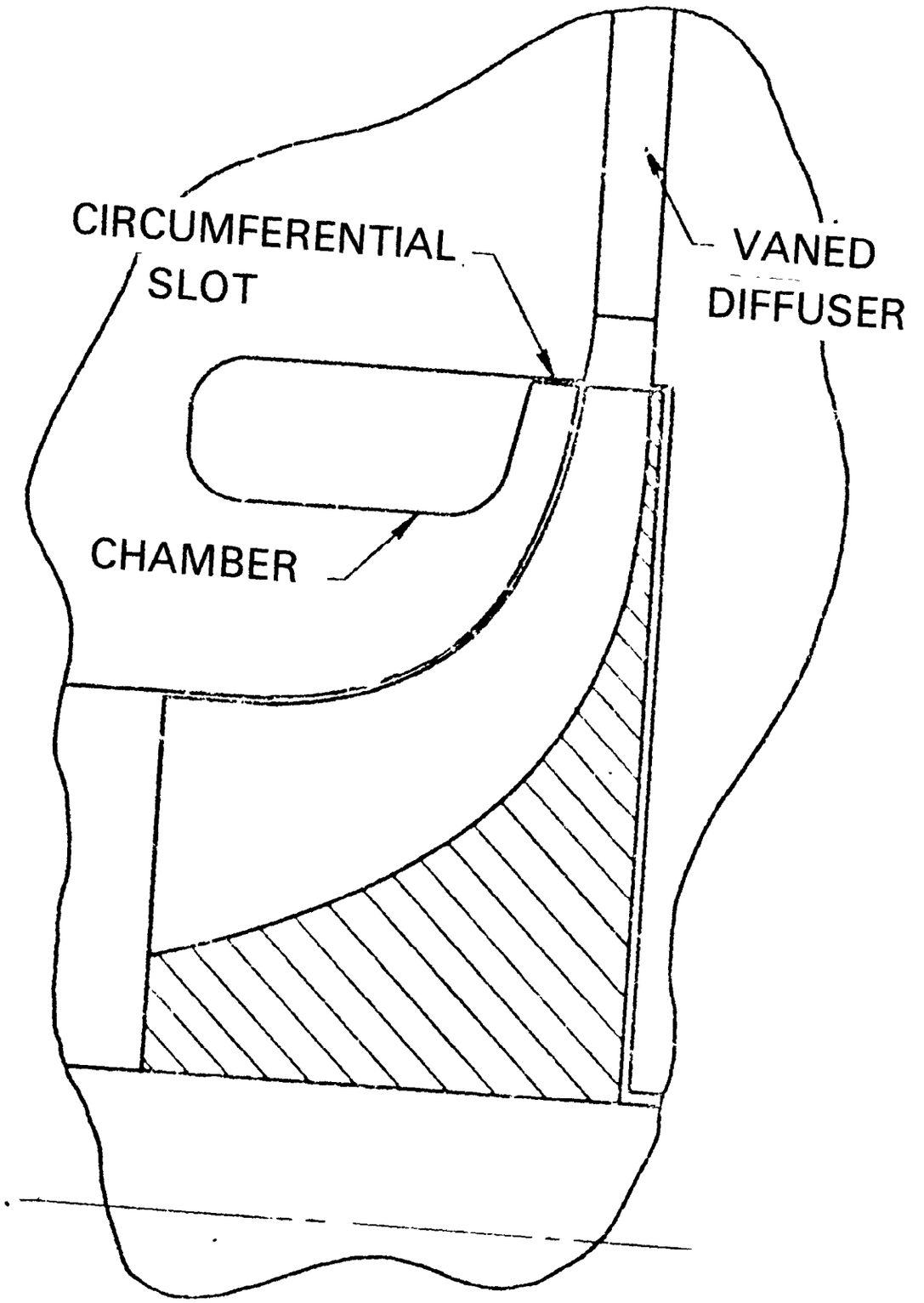

FIG.28 CIRCUMFERENTIAL SLOT AND CHAMBER FOR SURGE MARGIN IMPROVEMENT (AMANN, REF 28)

SK 117649

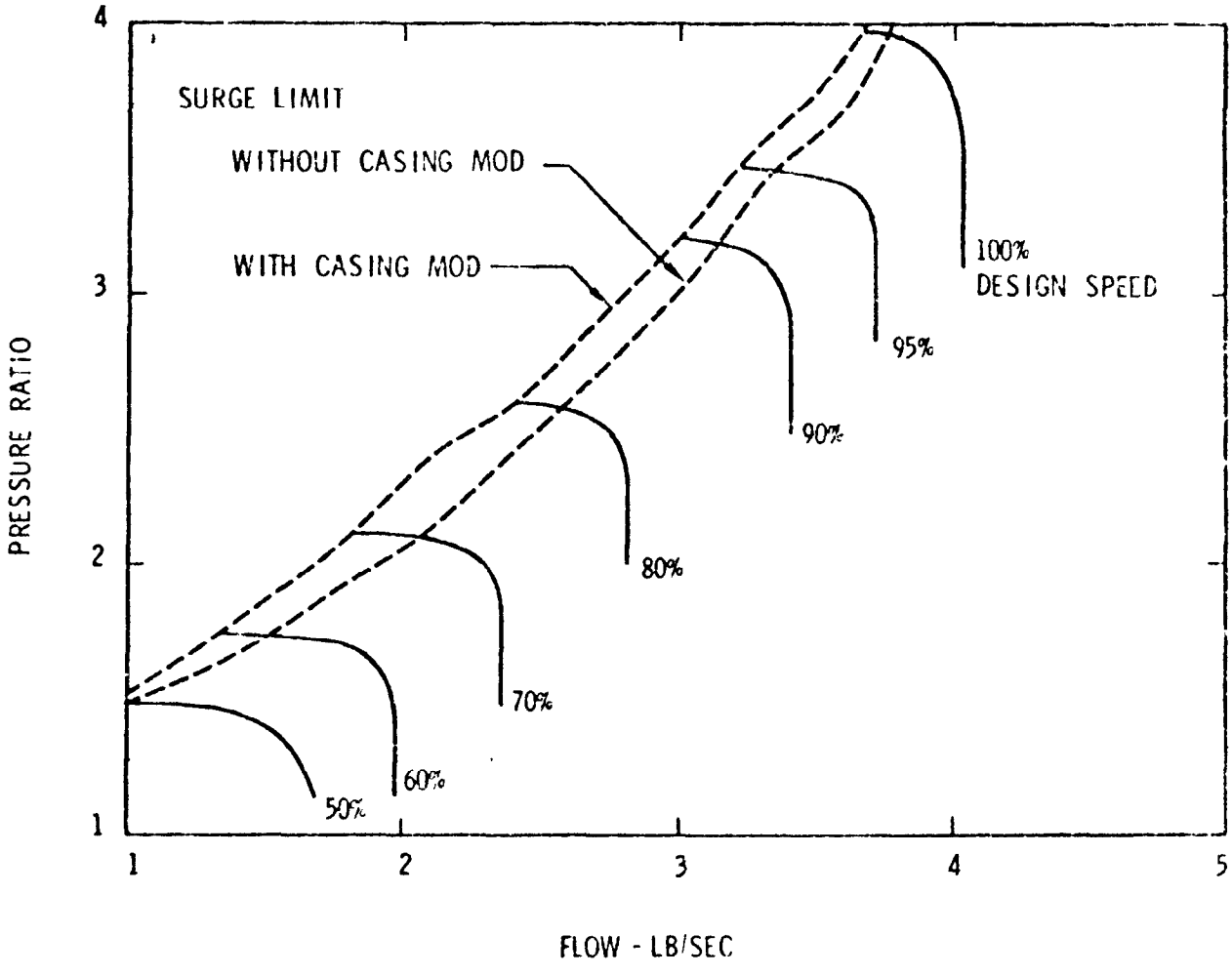

FIG.29 EFFECT OF CIRCUMFERENTIAL SLOT ON SURGE MARGIN (AMANN, REF 31)

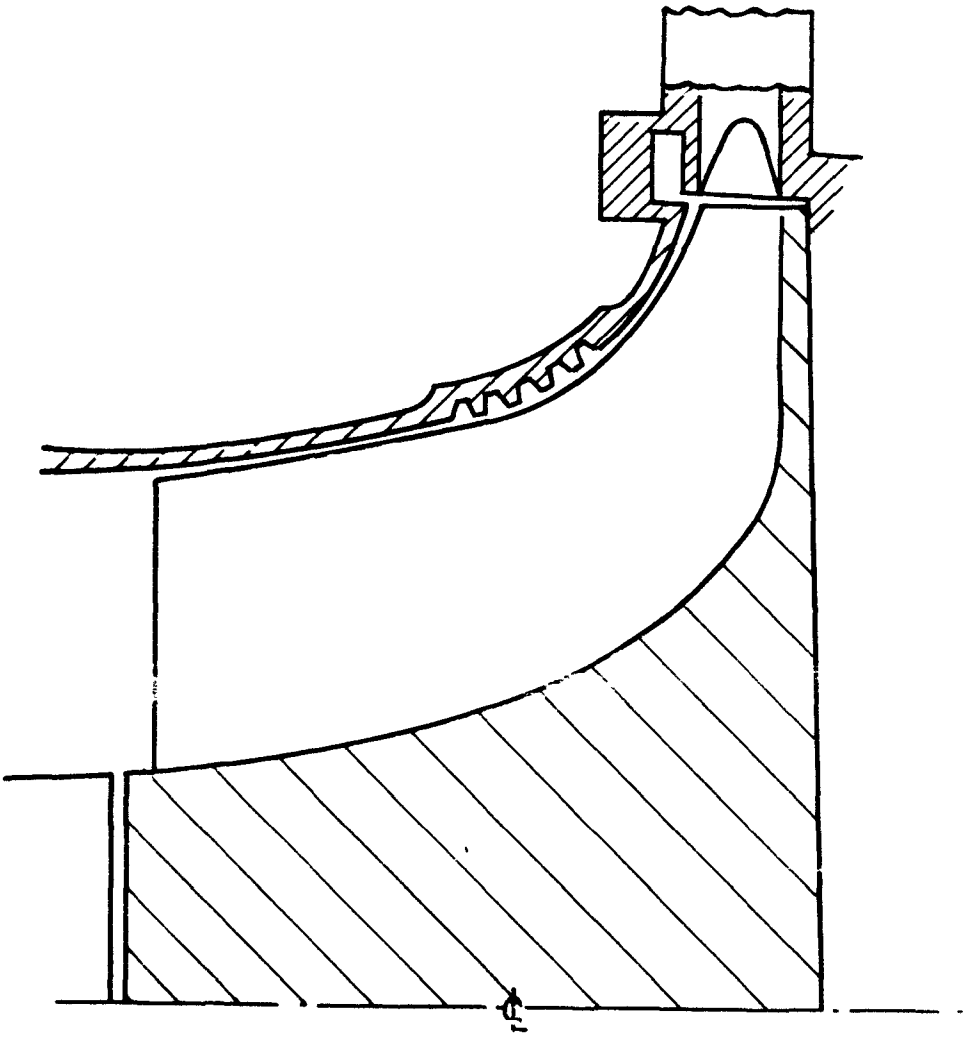

FIG. 30 U.A.C. SHROUD CASING GROOVES

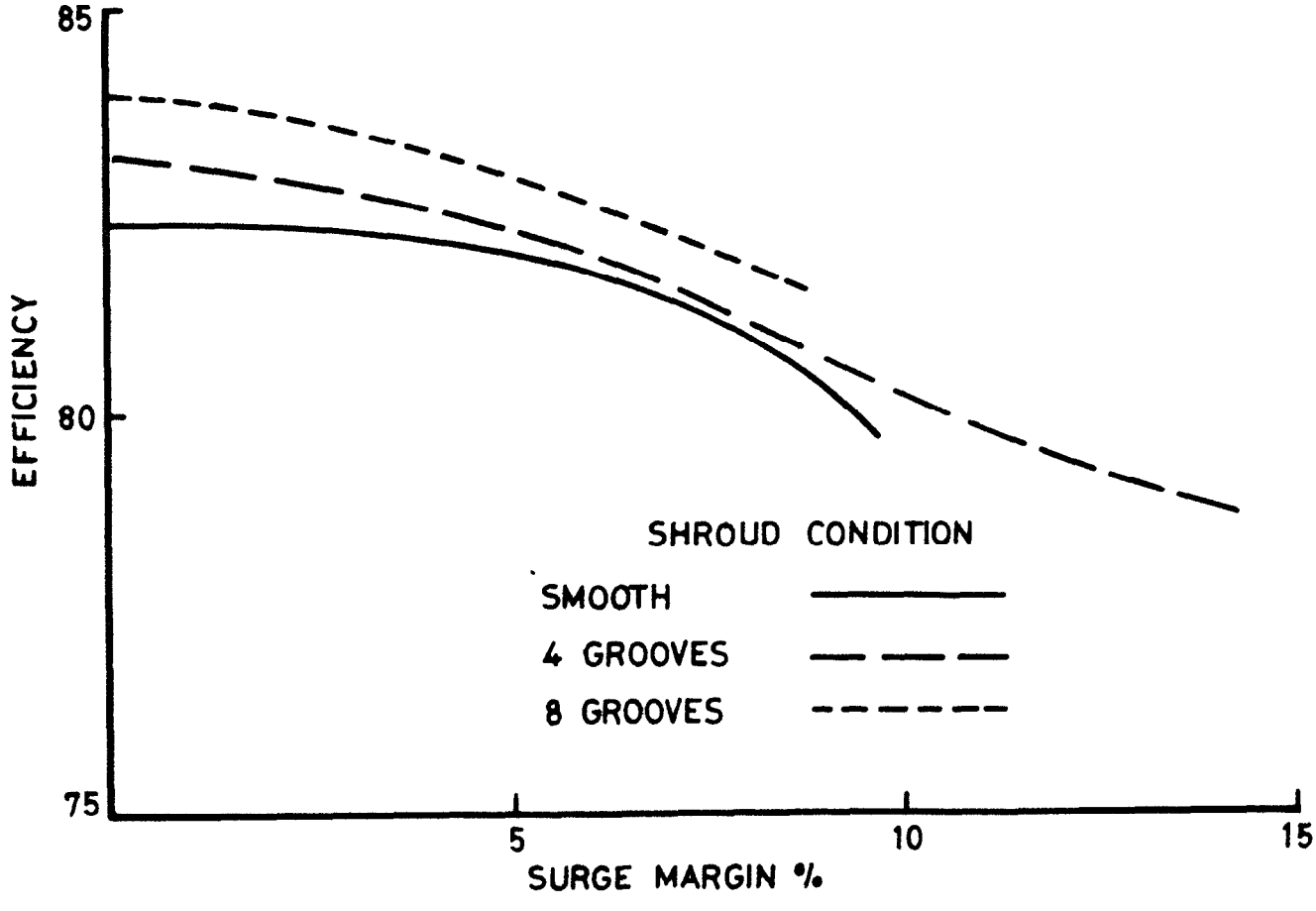

FIG. 31 U.A.C. GROOVES-EFFECT ON PERFORMANCE

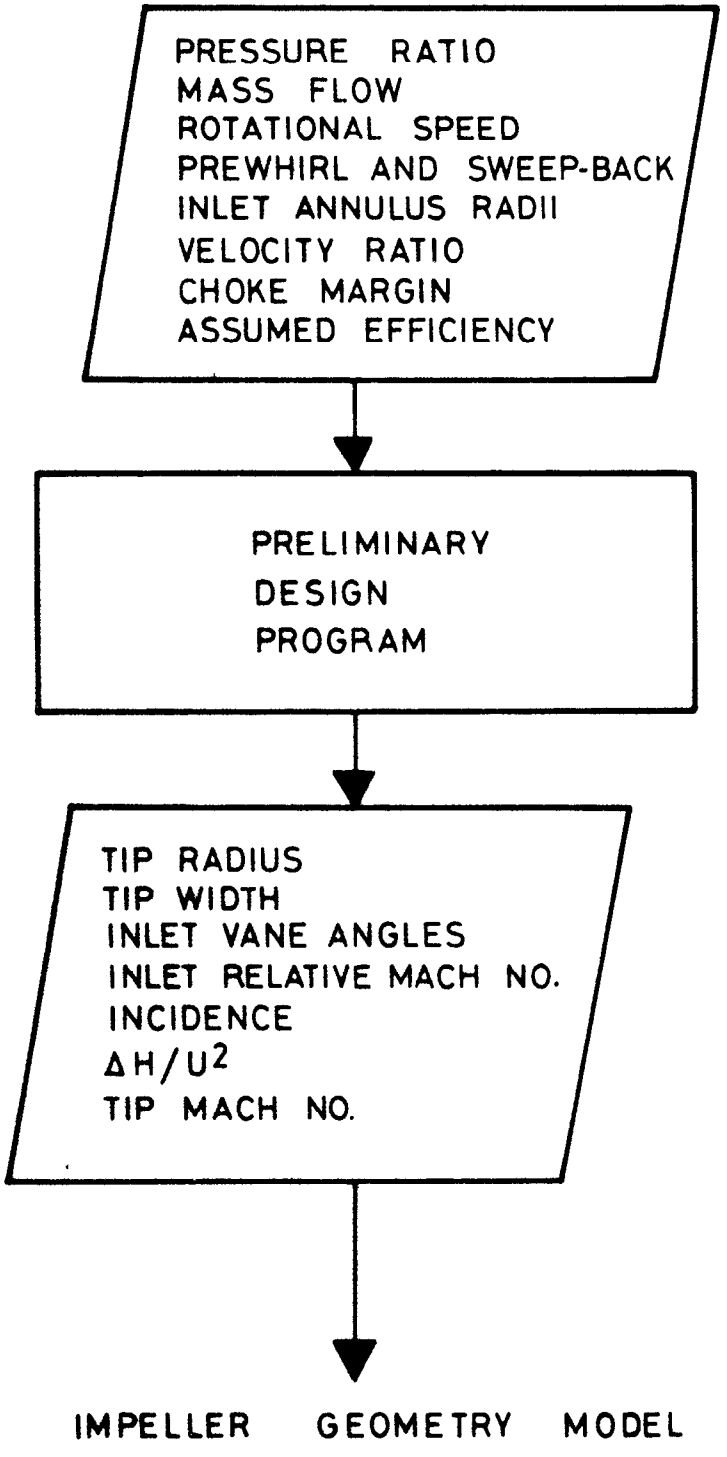

FIG. 32 PRELIMINARY DESIGN PROGRAM

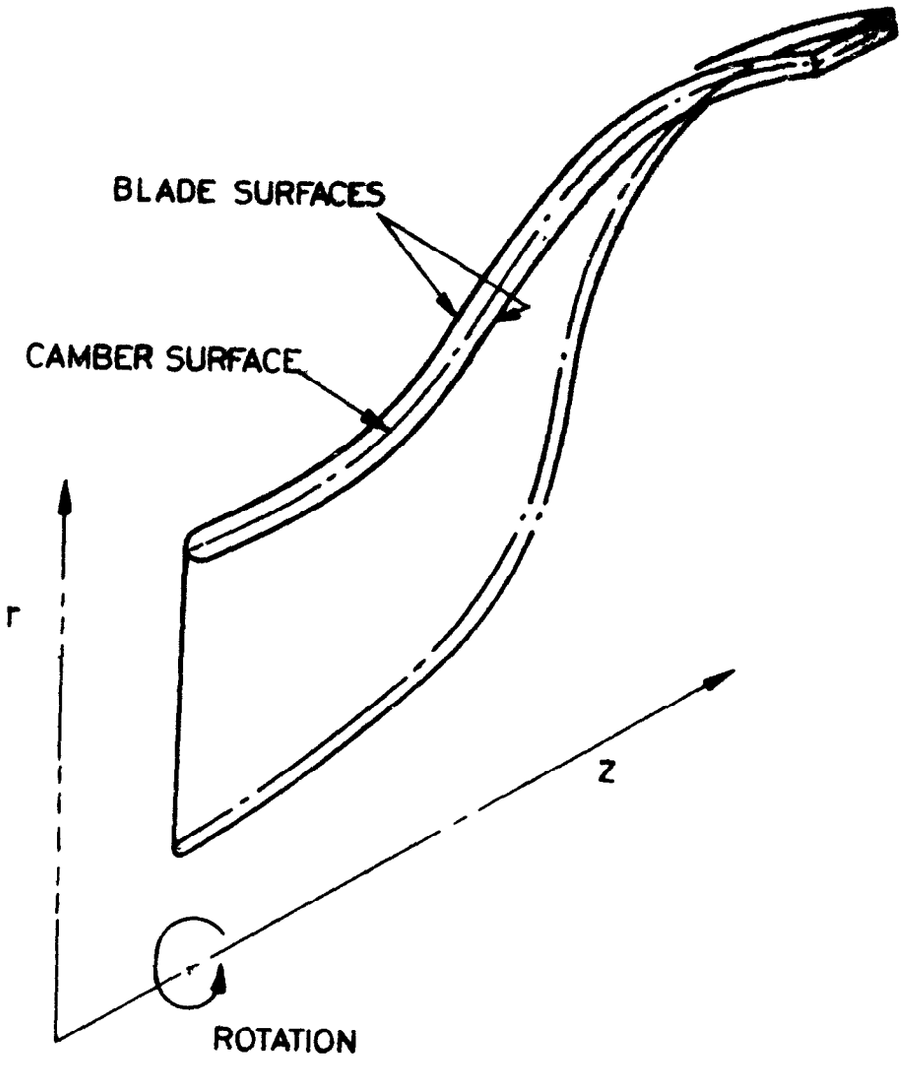

FIG.33 ANALYTIC SURFACES USED TO DEFINE THE VANES OF IMPELLERS

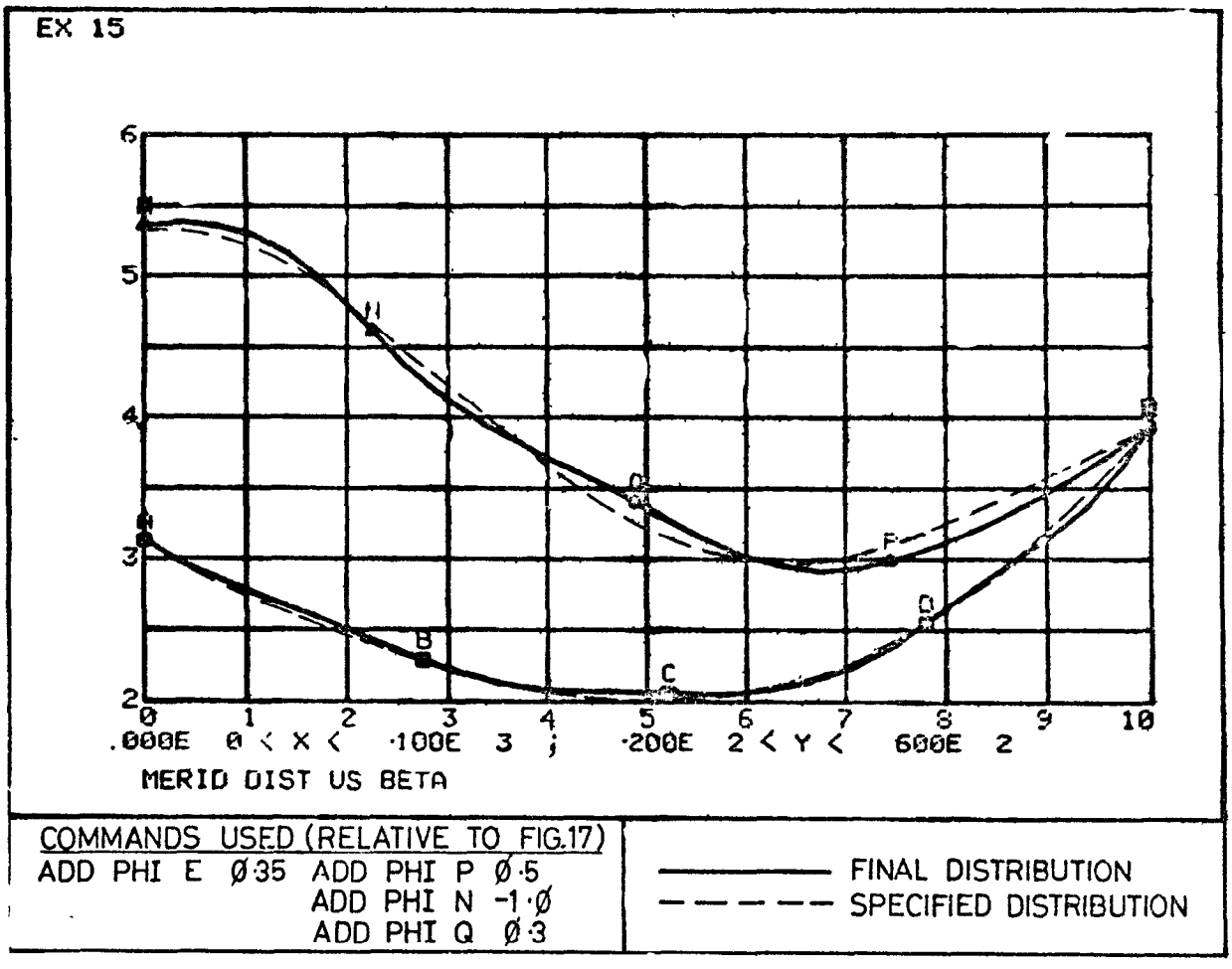

FIG.34 STORAGE TUBE DISPLAY OF CAMBER DISTRIBUTION

SK 117884

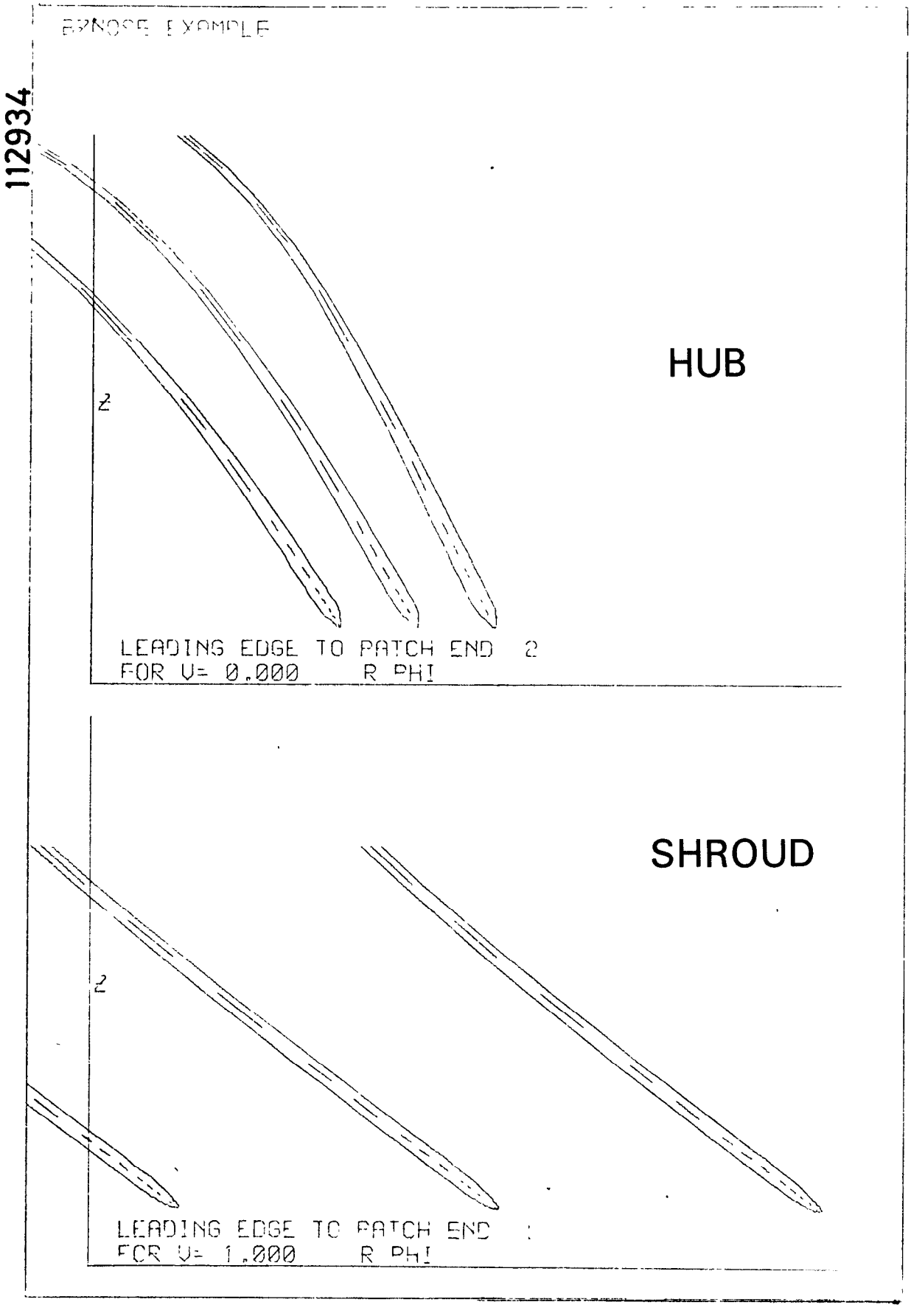

FIG.35 STORAGE TUBE DISPLAY OF INDUCER

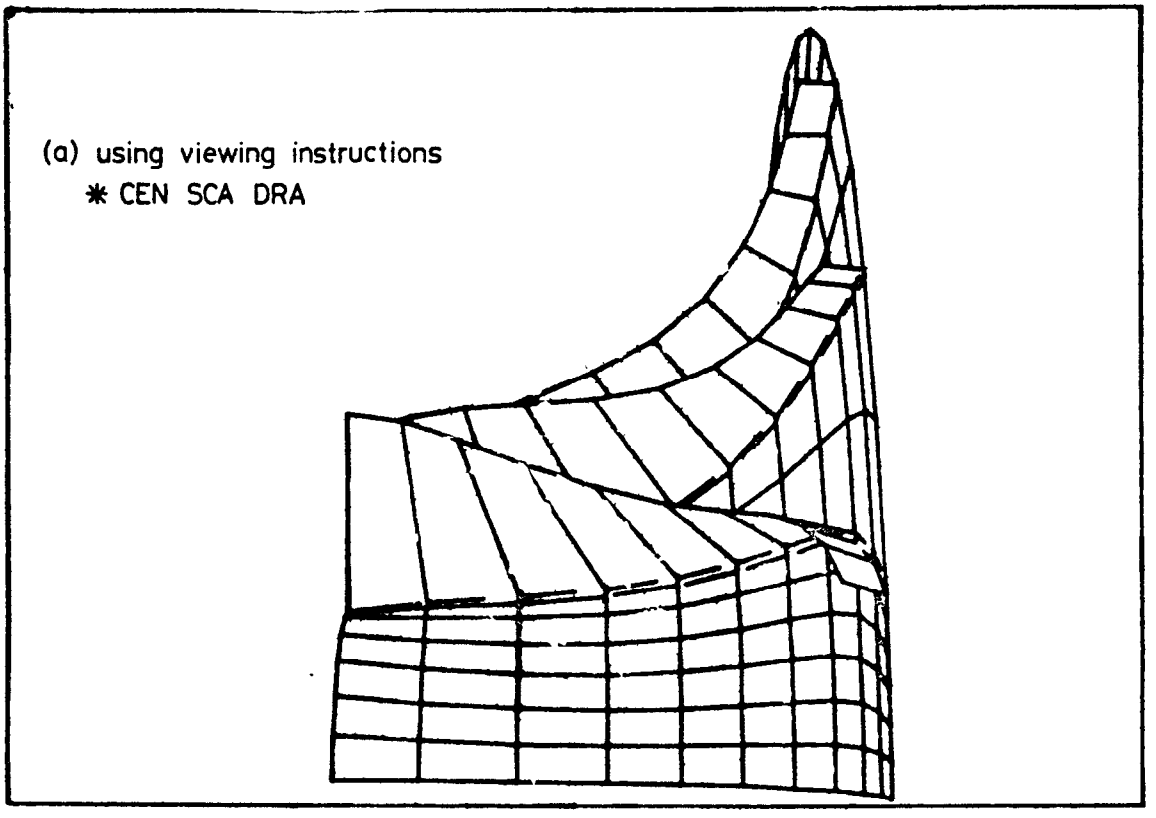

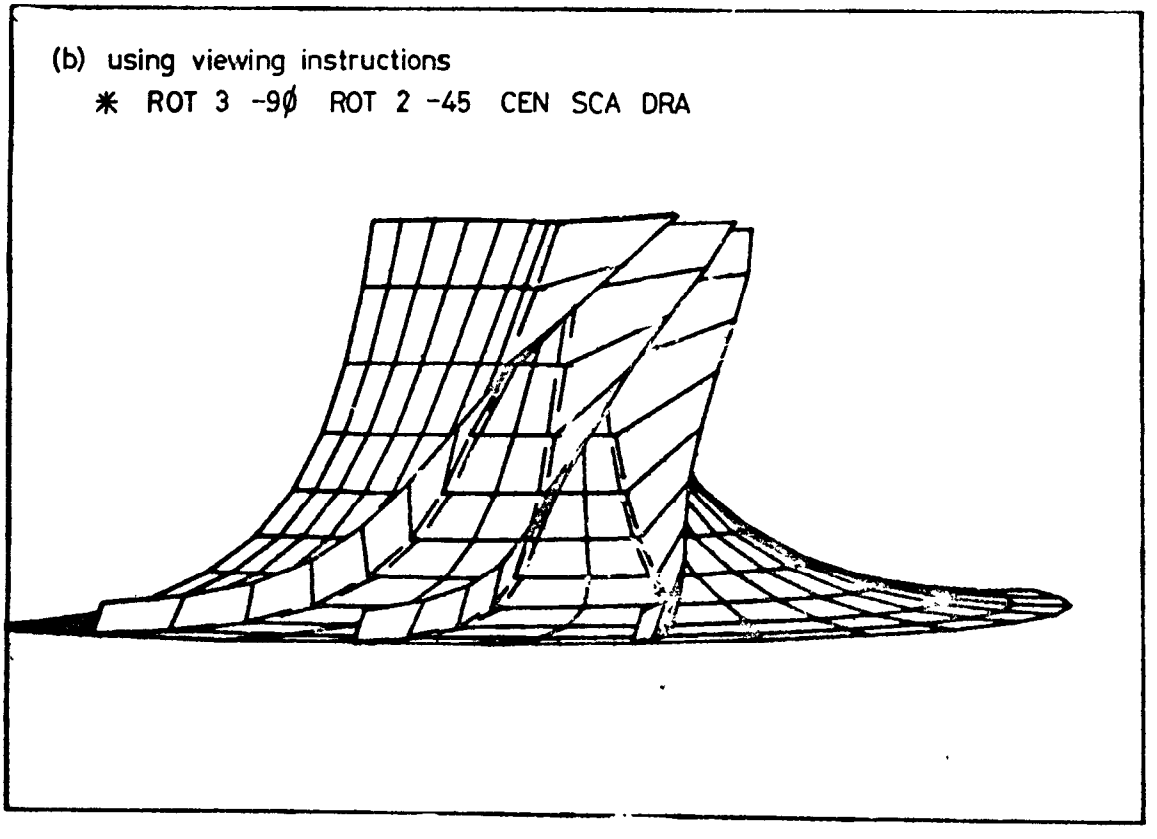

FIG.36 STORAGE TUBE DISPLAY OF PERSPECTIVE VIEWS OF IMPELLER

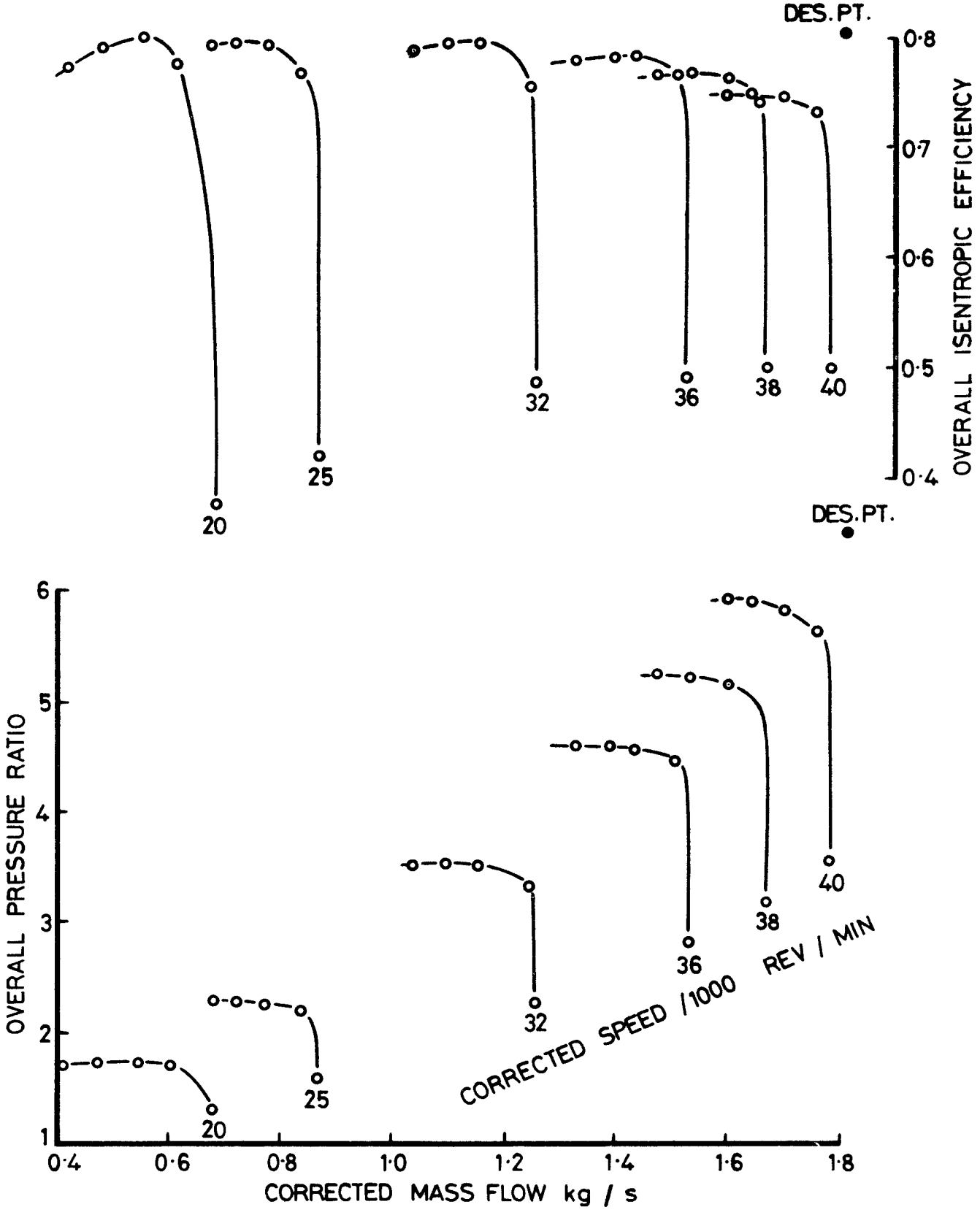

FIG. 37. EXPERIMENTAL CHARACTERISTICS OF COMPRESSOR 'A'

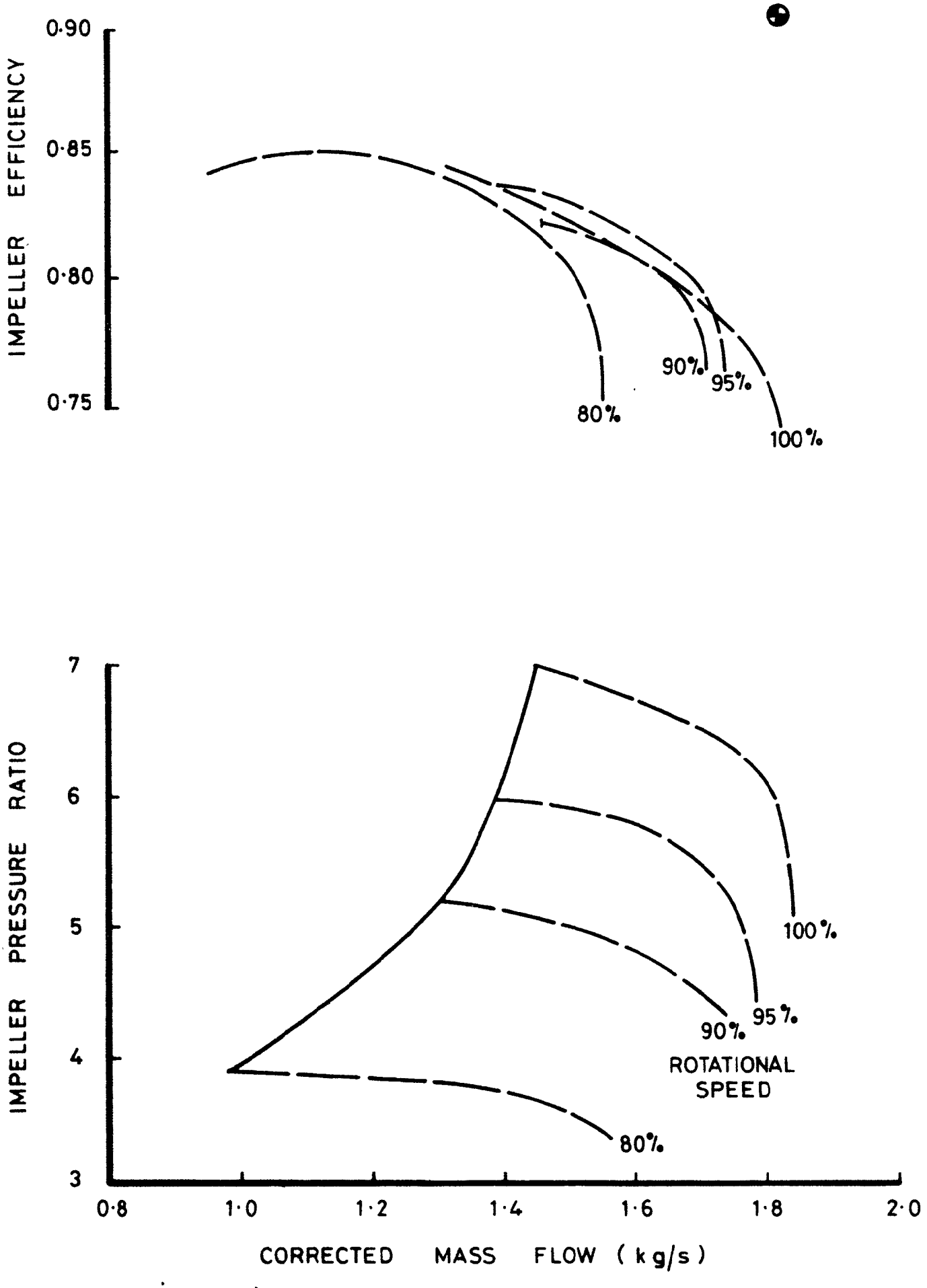

FIG. 38 · COMPRESSOR 'A' ~ IMPELLER ALONE PERFORMANCE

117840

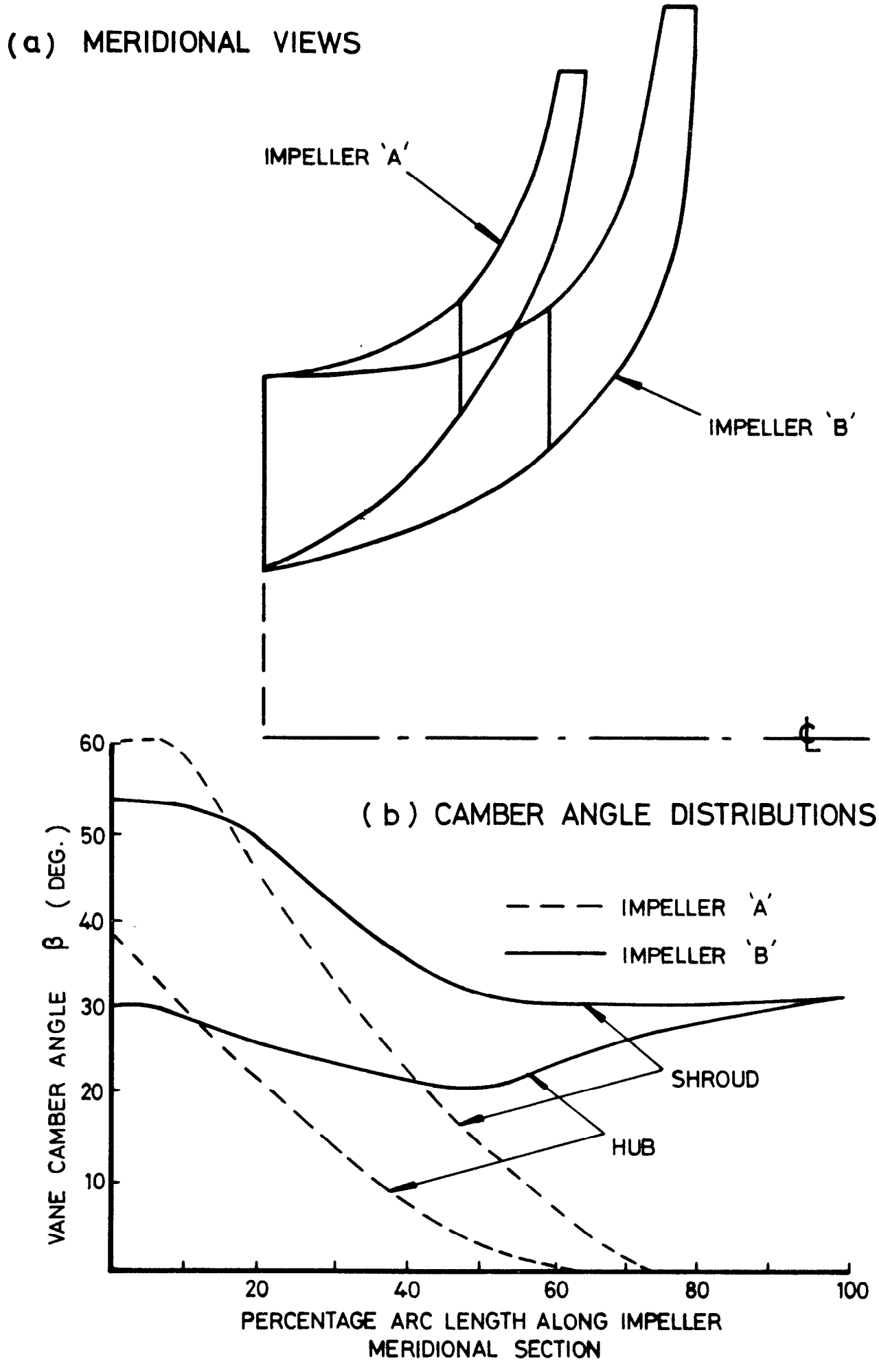

FIG.39. GEOMETRIC COMPARISON OF IMPELLER 'A' AND IMPELLER 'B'

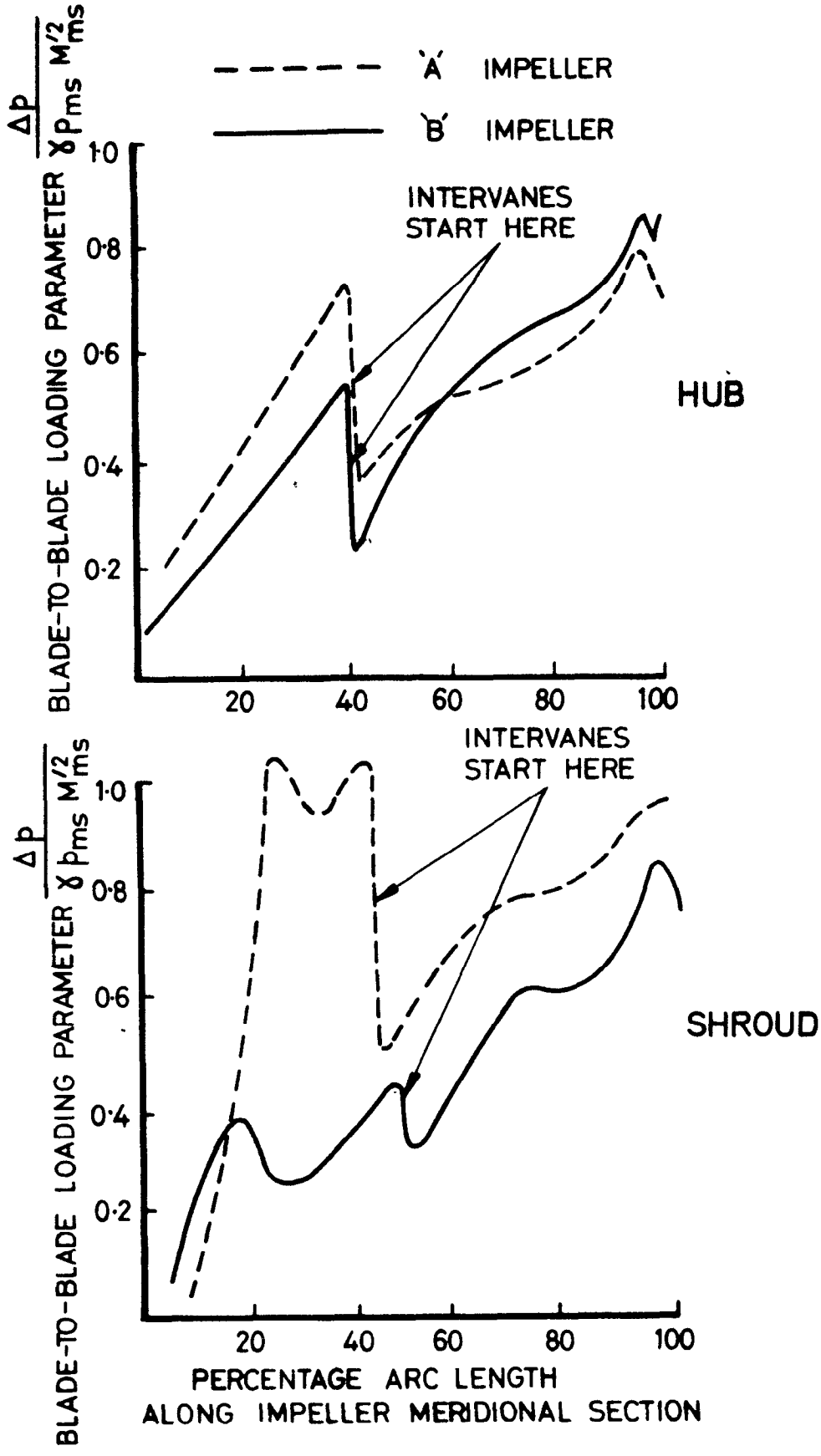

FIG 40 DISTRIBUTIONS OF BLADE-TO-BLADE LOADING FOR IMPELLERS 'A' AND 'B'

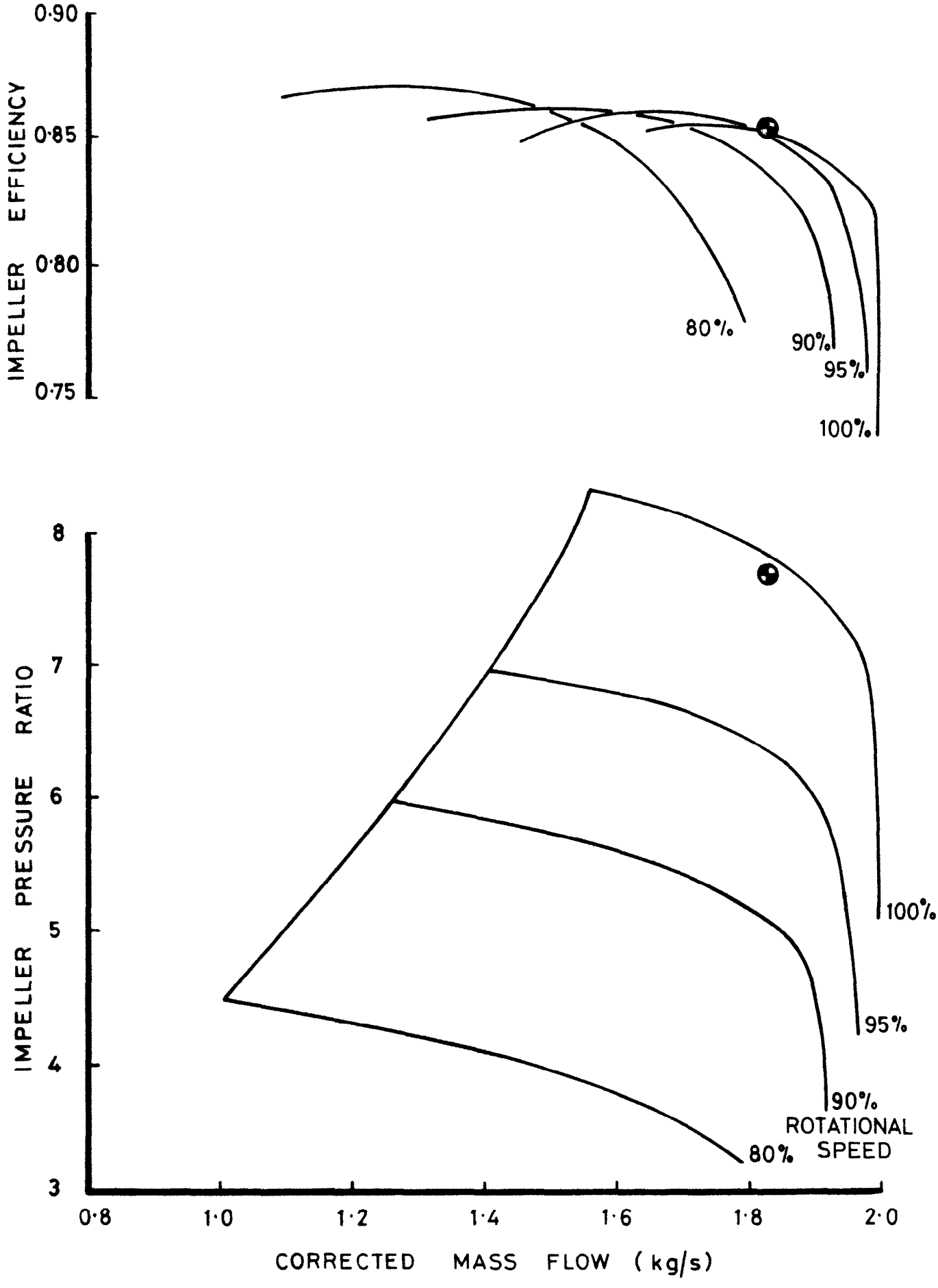

FIG. 41 COMPRESSOR 'B' ~ IMPELLER ALONE PERFORMANCE

Produced in England by Her Majesty's Stationery Office, Reprographic Centre, Basildon
[illegible] 00544/290279 K4 3/77 PQ3

ARC CP No.1363
July 1976

Came, P.M.

THE CURRENT STATE OF RESEARCH AND DESIGN IN HIGH PRESSURE RATIO CENTRIFUGAL COMPRESSORS

A review of the achievements of research effort in centrifugal compressors is presented and its effect on current design methods is discussed. The paper concludes with recommendations for future research.

ARC CP No.1363
July 1976

Came, P.M.

THE CURRENT STATE OF RESEARCH AND DESIGN IN HIGH PRESSURE RATIO CENTRIFUGAL COMPRESSORS

A review of the achievements of research effort in centrifugal compressors is presented and its effect on current design methods is discussed. The paper concludes with recommendations for future research.

ARC CP No.1363
July 1976

Came, P.M.

THE CURRENT STATE OF RESEARCH AND DESIGN IN HIGH PRESSURE RATIO CENTRIFUGAL COMPRESSORS

A review of the achievements of research effort in centrifugal compressors is presented and its effect on current design methods is discussed. The paper concludes with recommendations for future research.

ARC CP No.1363
July 1976

Came, P.M.

THE CURRENT STATE OF RESEARCH AND DESIGN IN HIGH PRESSURE RATIO CENTRIFUGAL COMPRESSORS

A review of the achievements of research effort in centrifugal compressors is presented and its effect on current design methods is discussed. The paper concludes with recommendations for future research.

DETACHABLE ABSTRACT CARDS

HER MAJESTY'S STATIONERY OFFICE

Government Bookshops

49 High Holborn, London WC1V 6HB
13a Castle Street, Edinburgh EH2 3AR
41 The Hayes, Cardiff CF1 1JW
Brazennose Street, Manchester M60 8AS
Southey House, Wine Street, Bristol BS1 2BQ
258 Broad Street, Birmingham B1 2HE
80 Chichester Street, Belfast BT1 4JY

Government publications are also available through booksellers

C.P. No. 1363

ISBN 0 11 470999 8